

Final report
on the regional key comparison Euromet.M.P-K1.b
(Euromet Project 442, Phase B)
in the pressure range from $3 \cdot 10^{-4}$ Pa to 0.9 Pa

Karl Jousten¹, Mercede Bergoglio², Anita Calcatelli², Jean-Noel Durocher³, John Greenwood⁴, Rifat Kangi⁵, Jean-Claude Legras³, Carmen Matilla⁶, Janez Setina⁷

August 2004

¹ Physikalisch-Technische Bundesanstalt (PTB), Abbestr. 2-12, 10587 Berlin, Germany

² Istituto Metrologia Gustavo Colonnetti (IMGC-CNR), Strada delle Cacce 73, 10135 Torino, Italy

³ BNM-LNE, 1, rue Gaston Boissier, 75724 Paris Cedex 15, France

⁴ National Physical Laboratory (NPL), Queen Road Teddington, Middlesex, United Kingdom TW11 0LW

⁵ TUBITAK - Ulusal Metroloji Enstitüsü (UME), Gebze, 41470, Kocaeli, Turkey

⁶ Centro Espanol de Metrologia (CEM), Calle del Alfar, 2, 28760 Tres Cantos – Madrid, Spain

⁷ Institute of Metals and Technology (IMT), Lepi Pot 11, 1000 Ljubljana, Slovenia

Content

1. INTRODUCTION	3
2. PARTICIPATING LABORATORIES AND THEIR STANDARDS	3
2.1. CALIBRATION SYSTEM AT THE BNM-LNE	5
2.2. CALIBRATION SYSTEM AT THE CEM	5
2.3. CALIBRATION SYSTEM AT THE IMT	5
2.4. PRIMARY STANDARDS OF THE IMGCC-CNR	6
2.5. STATIC EXPANSION SYSTEM OF THE NPL	7
2.6. STATIC EXPANSION SYSTEM OF THE PTB (PILOT LABORATORY)	7
2.7. STATIC EXPANSION SYSTEM OF THE UME	7
3. TRANSFER STANDARDS	8
4. CALIBRATION CONSTANT	9
5. ORGANISATION OF THE COMPARISON AND CHRONOLOGY	10
6. CALIBRATION PROCEDURE AND RESULTS TO BE REPORTED.....	11
7. UNCERTAINTIES OF REFERENCE STANDARDS.....	13
8. UNCERTAINTIES OF REPORTED MEASURED VALUES	14
9. REPORTED RESULTS OF EACH LABORATORY	17
10. STABILITY OF TRANSFER GAUGES.....	20
11. DATA REDUCTION AND GENERATING A COMMON REFERENCE VALUE	22
12. LINK TO KEY COMPARISON CCM.P-K4.....	32
13. DISCUSSION AND CONCLUSIONS	36
14. APPENDIX	37
15. REFERENCES	38

1. Introduction

At the Euromet Vacuum Workshop held at NPL on October 8, 1997, it was decided to carry out comparisons in two vacuum pressure ranges: from 0.1 Pa to 1000 Pa (Phase A) and from 10^{-4} Pa to 1 Pa (Phase B). These comparisons were organised in the frame of the Euromet Project 442, where the first of these pressure ranges (Phase A) was started in summer 1999, the second (Phase B) was started in spring 2000. For phase B, the Laboratory for Vacuum Metrology at PTB was chosen as the pilot laboratory. In consideration of the accuracy of the available transfer standards, the pressure range of Phase B was specified to $3 \cdot 10^{-4}$ Pa ... 0.9 Pa. This comparison was later listed as key comparison Euromet.M.P-K1.b in the BIPM data base .

The objective of the comparison was to determine the degree of equivalence of absolute pressure standards within Euromet. In addition to the measurand, the crucial value for the determination of the degree of equivalence is the uncertainty of the generated pressure in the calibration standard. This value was considered as solely the responsibility of the participating laboratories and had to be reported as part of the calibration report. In contrast, all additional uncertainties that were related to the transfer standard were evaluated by the pilot laboratory in order to have a uniform uncertainty analysis for all participants and in order to emphasize the importance of the reported uncertainty of the generated pressure.

Since three of the participants took part in key comparisons organised by CCM in overlapping pressure ranges, the comparison also allows the possibility of finding deviations from the CCM reference value for each participant for a part of the pressure range under consideration. It is therefore the regional continuation of a key comparison.

Two spinning rotor gauges were chosen as transfer standards, which were to be calibrated at the following target pressures (nitrogen gas): $3 \cdot 10^{-4}$ Pa, $9 \cdot 10^{-4}$ Pa, $3 \cdot 10^{-3}$ Pa, $9 \cdot 10^{-3}$ Pa, $3 \cdot 10^{-2}$ Pa, $9 \cdot 10^{-2}$ Pa, 0.3 Pa, and 0.9 Pa.

2. Participating laboratories and their standards

Table 1 lists the laboratories that participated in this comparison in alphabetic order. One laboratory, the Slovak Institute of Metrology (SMU), did participate in the comparison, but delivered no calibration results to the pilot laboratory and was therefore deleted from the list. Another laboratory, the Czech Metrological Institute (CMI), withdrew all its data after the comparison and was deleted from the list as well.

In the second column of Table 1, the standards used for the calibration of the transfer standards are listed, in the third column it is characterised according to whether the standard is considered as primary or secondary, in the next column the traceability of the standard is given, the fifth column indicates, if the laboratory was listed in the CMC tables of the BIPM in the relevant pressure range at the time of the comparison.

Table 1 List of participants in alphabetic order and the standards used for the calibration of the transfer standards.

Laboratory	Standard	Character of standard	Traceable to:	CMC listed
BNM-LNE France	Spinning rotor gauge	Secondary	independent	yes
Centro Espanol de Metrologia (CEM) Spain	2 Spinning rotor gauges	Secondary	PTB	yes
Institute of Metals and Technology (IMT) Slovenia	Spinning rotor gauge	Secondary	independent	no
Istituto Metrologia Gustavo Colonnetti (IMGC-CNR) Italy	Continuous expansion system (< 0,3 Pa) Static expansion system	Primary	independent	yes
National Physical Laboratory (NPL) United Kingdom	Static expansion system	Primary	independent	yes
Physikalisch-Technische Bundesanstalt (PTB) Germany	Static expansion system	Primary	independent	yes
TUBITAK - Ulusal Metroloji Enstitusu (UME) Turkey	Static expansion system	Primary	independent	yes

Mainly two types of standards were involved in the comparison: Static expansion systems as primary standards (4 laboratories) and spinning rotor gauges (SRG) as reference or secondary standards (3 laboratories). The BNM-LNE and the IMT were able to calibrate these secondary standards in their own facilities and can therefore be considered as independent. The IMT used a newly designed static expansion system to calibrate its reference SRG, for the initial pressure measurement of the system, however, an instrument traceable to the IMGC-CNR was used. This link is of minor importance, since it does not contribute largely to the uncertainty of the standard.

The IMGC-CNR used the static expansion system for the upper pressure range (0.3 Pa and 0.9 Pa), but a continuous expansion system for pressures below this range.

2.1. Calibration system at the BNM-LNE

The BNM-LNE standard is a combination of three devices: a 100 Pa-range differential capacitance diaphragm gauge (CDG), a spinning rotor gauge (SRG) and an ion gauge. All the instruments to be compared were connected symmetrically to a 66 L vacuum chamber. The CDG was initially calibrated at a line pressure near 50 kPa by comparison with two primary pressure balances the effective area of which is 20 cm². Then the reference chamber was evacuated using a turbomolecular pump. The thermal transpiration effect is corrected by using the Takaishi and Sensui formulas [1] with the sensor temperature determined experimentally. The accommodation coefficient of the SRG was determined by comparison with the CDG in the range 0.05 Pa to 5 Pa. The offset of the SRG was calculated by combining the information from the SRG and the ion gauge.

At each step of establishment of the pressure scale, the extrapolation was checked by circular comparison between several CDGs and SRGs. The validity of the method was demonstrated in the range 1·10⁻³ Pa to 100 Pa using the static expansion method: the correspondence of a quartz manometer, a CDG and two SRGs was inside 0.2 %.

2.2. Calibration system at the CEM

The CEM's pressure standard is based on the continuous expansion method. Although the system is already working, during this intercomparison it was used as a comparison calibration system.

The results were obtained by direct comparison between the reference pressure readings and the readings of the transfer devices. The reference pressure was established by using two Spinning Rotor Gauges manufactured by MKS, with the MKS SRG-2CE model controller, traced to PTB. Simultaneously, a MKS CDG (1 torr) was used as a check standard. Their indications were recorded together with the temperature of the chamber. The base pressure was determined by using an ionisation gauge.

2.3. Calibration system at the IMT

Calibrations were performed on the main chamber of the newly developed static expansion calibration system (SE1) at IMT. The chamber has a cylindrical shape with a diameter of 150 mm and height of 320 mm. The volume of the chamber is approximately 5.8 L. It has eight CF35 connection ports for vacuum gauges, located in two planes. The calibration method was direct comparison with a reference spinning rotor gauge, which had been calibrated "in-situ"

by static expansion just before Project 442 measurements. The transfer standards and reference SRG were connected to two opposite ports in the upper plane (symmetrically with respect to the chamber axis and at the same height). The calibration pressure for direct comparison was established by a stationary equilibrium for pressures below 0.09 Pa, and statically at 0.09 Pa and above. The gas inlet for calibrations by comparison was made via the connection tube (diameter 35 mm) between the calibration chamber and the pumping system. A turbomolecular pump was used to evacuate the system.

2.4. Primary standards of the IMGC-CNR

At IMGC-CNR two primary standards were used: The continuous expansion system up to 0.09 Pa, the static expansion system for 0.3 Pa and 0.9 Pa.

The IMGC-CNR continuous expansion system is based on the expansion of a pure gas, which is pumped through a fixed conductance. The fixed conductance was evaluated by both analytical and Monte Carlo methods. The effective pumping speed is computed from the values of calculated conductance and the ratio of the conductance to the pumping speed is periodically measured. The gas flow-rate device used to generate the pressures into the fixed conductance IMGC-CNR-D2 system is based on the constant pressure-variable volume method. The upper limit of the molecular range of the system was defined from pressure measurements and is below 10^{-1} Pa. At the time of the comparison, the relative standard uncertainty in the total working range, that is from 10^{-6} Pa to 10^{-1} Pa, varied from $9.8 \cdot 10^{-3}$ to $2.0 \cdot 10^{-3}$ including the repeatability of the generated pressure measurements.

The static expansion system at the IMGC-CNR is a modification of that described in reference [2], the principal difference being the addition of a third volume as described in reference [3]. The system consists of three volumes, nominally 10 mL, 500 mL and 50 L, the largest volume being the calibration chamber. The different expansion ratios are measured, and are periodically determined, by application of the multiple-expansion method. The initial pressures between 1 kPa and 100 kPa are measured by secondary transfer standards directly traceable to the HG5 mercury manometer. The base pressure, which is obtained by a turbo pump, is in the range of 10^{-6} Pa. The relative combined uncertainty of the system for the pressure range 0.1 Pa to 100 Pa is $2.1 \cdot 10^{-3}$ when volumes added to the system by gauges to be calibrated can be disregarded.

2.5. Static expansion system of the NPL

The NPL standard SEA2 is a stainless steel, UHV compatible, series expansion apparatus in which calculable pressures between $5 \cdot 10^{-7}$ Pa and 900 Pa may be generated.

In operation, a sample of gas is trapped in one of the small vessels and then expanded into the next large and small vessels, which have previously been evacuated to a low pressure. This procedure is then repeated using subsequent expansion stages until the gas is expanded into the calibration vessel. The pressure of the initial gas sample is measured using a calibrated quartz Bourdon tube gauge. By varying the initial pressure and the number of expansion stages, a range of calibration pressures may be generated in the calibration vessel. The pressure generated is calculated from knowledge of the initial pressure, the gas temperature and the ratio of the relevant volumes.

The vacuum standard used during this comparison was not able to achieve one of the calibration pressures due to a gap in its operating range near to $3 \cdot 10^{-2}$ Pa. The closest pressure that could be achieved in this case was $2 \cdot 10^{-2}$ Pa.

2.6. Static expansion system of the PTB (pilot laboratory)

The primary standard of the PTB is a static expansion system, called SE1, in which pressures are generated by expanding gas of known pressure from a very small volume V_4 of 17 mL directly into a volume of 233 L, or by two successive expansions from a volume $V_1 = 17$ mL into an intermediate volume of 21 L including V_4 and then from V_4 into the 233 L vessel. The regular operational range of SE1 is 10^{-6} Pa up to 1 Pa. Due to the relatively high volume ratios, the initial pressure must be reduced below 1 kPa in the calibration sequence of this comparison, when for $9 \cdot 10^{-3}$ Pa one expansion instead of two at lower pressures is performed. For this reason the uncertainty of the initial pressure measurement is higher and contributes significantly in an intermediate pressure regime (see Section 7). The system is described in more detail in references [4] and [5].

2.7. Static expansion system of the UME

A newly constructed multi-stage static expansion system has been used for generating calibration pressures in the range from $9 \cdot 10^{-4}$ Pa up to $9 \cdot 10^{-1}$ Pa. The apparatus consists of 6 vessels that provide a pressure reduction by a factor of about 10^{-6} in the main calibration vessel after three-step expansion. 17 platinum resistance thermometers mounted on the vessels are used to determine corrections for temperature effects. The initial pressure before

the first expansion is measured by an absolute quartz Bourdon spiral gauge (Ruska DPG 7000) having 172 kPa full scale. The whole apparatus is UHV compatible and can be baked up to 400° C. The relative standard uncertainties ($k = 1$) of pressures generated by this new standard range from $2.6 \cdot 10^{-3}$ at 10^{-3} Pa to $1.3 \cdot 10^{-3}$ at 10^3 Pa.

3. Transfer standards

Two spinning rotor gauges (SRG) have been chosen for the comparison. The SRG [6] is widely accepted as a transfer standard [7] due to its measurement accuracy and long-term and transport stability [8], [9]. Two devices were used in order to further reduce the influence of transport-instabilities, to produce redundancy, and to increase the accuracy of the comparison.

Only one controller for the two spinning rotor gauges was circulated, because participating laboratories had a spare controller available, so that in most cases the two transfer gauges could be calibrated at the same time on the same standard. To date there is no published evidence to indicate that a different controller and gauge head would have an influence on the calibration results of a rotor/finger combination.

PTB prepared and pre-tested the two spinning rotor gauges (Table 2). Rotor 1 was an etched stainless steel ball, with a nominal diameter of 4.762 mm, embedded in a 8 mm OD tube (“finger”) with a DN16 CF flange, numbered 25UM. Rotor 2 was an INVAR ball, with a nominal diameter of 4.50 mm, located in a similar finger, numbered 23UM.

Each finger was sealed with a special all metal valve [8] which had two functions: 1. To seal the rotor in the finger so that it could be transported under vacuum. 2. To fix the rotor during transportation so that the surface would not be changed due to milling and friction effects of the rolling ball.

Transport under vacuum required that the valve was only opened when it was connected to high vacuum and, before transportation, the valve was closed under high vacuum conditions. To ensure free spinning of the rotor the valve had to be completely opened.

Table 2 Transfer standards used for the comparison

Transfer standard	Rotor 1	Rotor 2
Material	Etched stainless steel	Invar
Nominal diameter	4.762 mm	4.5 mm
Nominal density	$7.715 \cdot 10^3 \text{ kg/m}^3$	$8.2 \cdot 10^3 \text{ kg/m}^3$

Data exists from 1994 onwards for calibration of each rotor at PTB. Both rotors showed a very good long-term stability of their effective accommodation coefficient with the relative

difference of the calibration constant not larger than 0.9% between the smallest and the largest value. Typical long-term instabilities per year were 0.2% for rotor 1 and 0.1% for rotor 2.

4. Calibration constant

The value to be calibrated by each laboratory j for each pressure for each rotor i was the effective accommodation coefficient σ_{ij} [6], often called σ_{eff} , which is mainly determined by the tangential momentum accommodation coefficient of the gas molecules to the rotor, and partly by the energy accommodation factor [6] and additionally by using nominal values for diameter and density of the rotors instead of the real ones.

σ_{ij} was determined by the following equation:

$$\sigma_{ij} = \sqrt{\frac{8kT_j}{\pi m} \cdot \frac{\pi d_i \rho_i}{20 p_{stj}} \left(\left(\frac{\dot{\omega}}{\omega} \right)_i - RD_i(\omega) \right)} \quad (1)$$

Herein p_{stj} is the generated pressure of nitrogen gas in the standard, T_j the temperature of gas in the calibration chamber, d_i and ρ_i are the (nominal) diameter and density of the rotor i , m is the molecular mass of nitrogen, $(\dot{\omega}/\omega)$, also called DCR, is the relative deceleration rate of the rotor frequency ω , and RD is a pressure independent residual drag, caused by eddy current losses in the surrounding metal structures and the rotor itself.

RD is generally a function of ω , $RD(\omega)$, so that it was required that, whenever σ_{ij} was determined, the value of ω also had to be measured in order to subtract the correct $RD(\omega)$ in Eq. (1). For measuring $RD(\omega)$ three options were offered by the comparison protocol.

Option 1: Before starting the calibrations the rotor frequency dependence of the residual drag (in unit $\text{DCR} = \text{s}^{-1}$) could be measured over a long period of time. The rotor frequency had to cover the full range that may occur during a calibration, that is normally $\omega/2\pi = 405 \text{ s}^{-1} \dots 415 \text{ s}^{-1}$, which may take 48 h. For this, the residual pressure in the standard must be below 10^{-6} Pa.

Option 2: It is possible to shorten the above measurement of the residual drag (offset) by intentionally letting gas into the vacuum system. After re-acceleration of the rotor to 415 s^{-1} , it was suggested to introduce 0.1 Pa of nitrogen gas and wait until the frequency drops to 412 s^{-1} , pump down to residual pressure and re-measure the offset. This procedure should be repeated for 409 s^{-1} , 406 s^{-1} , and 415 s^{-1} again to check the stability of the offset at one frequency. The whole sequence could be repeated several times to reduce the scatter of $RD(\omega)$.

Option 3: $RD(\omega)$ could be determined during the course of the calibrations by pumping down the vacuum system to residual pressure conditions after each target pressure point.

In all cases a linear least square fit had to be applied to obtain the function $RD(\omega)$.

Option 3 was the preferred option, since Options 1 and 2 require a high temperature stability of the laboratory over a long period of time due to the dependence of RD on temperature drifts. Option 3 was also recommended to check the data obtained by Options 1 or 2.

The determination of $RD(\omega)$ was considered as part of the calibration, because it affects its accuracy, and was the responsibility of each laboratory.

It is well known [6] that in the molecular regime up to about $3 \cdot 10^{-2}$ Pa σ_{eff} is pressure independent. For this reason, it was clear, a priori, that any pressure dependencies are likely to be due to measurement errors or problems of the calibration standard

In the protocol, no specific temperature for the calibration was requested. Unfortunately, after starting the comparison it was found [10] that σ_{eff} may be slightly dependent on the temperature of the rotor. For this reason we introduced an additional uncertainty for the pressures deduced from σ_{eff} (see Section 11 before Eq. (14) and after Eq. (15)), since calibrations were performed at different temperatures.

5. Organisation of the comparison and chronology

In order to reduce the effects of long-term and transport instabilities of the rotors, it was decided that after two or three participants the rotors were to be returned to the pilot laboratory for re-calibration. For the determination of the transport instability it was assumed that the primary standard of the pilot laboratory is stable. To substantiate this assumption the pilot laboratory used a third SRG (check standard), which was in all cases calibrated at the same time as the transfer gauges. This third check standard also served as a spare rotor in the case that one of the other rotors became faulty during the course of the comparison, which, fortunately, did not happen.

Table 3 presents the actual chronology of the calibrations including the calibrations of institutes that later did not deliver (SMU) or withdrew (CMI) results. Both at IMG-CNR and UME broken parts of their primary standards caused a change in the scheduled order. Customs problems in the Czech Republic due to an expired ATA Carnet caused a considerable delay of several months in the progress of the comparison.

Table 3 Chronology of measurements

Calibrating Laboratory	Date	Note
PTB 1	April 2000	As scheduled
NPL, UK	May 2000	As scheduled
LNE, France	June 2000	As scheduled
PTB 2	July 2000	As scheduled
IMI, Slovenia	September 2000	Order changed with IMGC-CNR
IMGC-CNR, Italy	October/November 2000	Delay at customs
SMU, Slovakia	December/February 2001	no calibration results delivered
PTB 3	March 2001	
CEM, Spain	April 2001	UME postponed as last
CMI, Czech Rep.	May to October 2001	Delay at CMI and customs. Data withdrawn.
PTB 4	November 2001	
UME, Turkey	December/January 2002	Order changed, because of broken pump at standard
PTB 5	February 2002	Comparison finished

6. Calibration procedure and results to be reported

The following calibration procedure was agreed upon before the comparison: Each laboratory was to calibrate the two SRGs at the following 8 nominal target pressures p_t for nitrogen pressure in ascending order: $3 \cdot 10^{-4}$ Pa, $9 \cdot 10^{-4}$ Pa, $3 \cdot 10^{-3}$ Pa, $9 \cdot 10^{-3}$ Pa, $3 \cdot 10^{-2}$ Pa, $9 \cdot 10^{-2}$ Pa, 0.3 Pa, 0.9 Pa.

A tolerance of $\pm 10\%$ in hitting the nominal pressure was accepted for $p_t < 9 \cdot 10^{-2}$ Pa and $\pm 5\%$ for $9 \cdot 10^{-2}$ Pa, 0.3 Pa, 0.9 Pa. Each target pressure had to be generated 3 times. This meant that in static expansion and comparison systems, after a measurement at the target point, the system was pumped down to residual pressure conditions and the same point re-generated, in continuous expansion systems it was sufficient to re-measure all quantities contributing to the calculated pressure. In total $8 \cdot 3 = 24$ points were measured in this way and were considered as one calibration sequence. It was required that this calibration sequence be repeated at least once on another day.

The readings of each of the SRGs were to be sampled in the following manner:

- 10 repeat points at 30 s intervals for the target points $3 \cdot 10^{-4}$ Pa, $9 \cdot 10^{-4}$ Pa, and $3 \cdot 10^{-3}$ Pa.
- 5 repeat points at 30 s intervals for $9 \cdot 10^{-3}$ Pa, $3 \cdot 10^{-2}$ Pa, $9 \cdot 10^{-2}$ Pa.
- 5 repeat points at 10 s intervals for 0.3 Pa and 0.9 Pa.

Regardless of the option chosen for offset determination, it was required that the offset be measured during the calibration:

- At the beginning of the calibration sequence
- After the target pressures $3 \cdot 10^{-4}$ Pa, $9 \cdot 10^{-4}$ Pa, $3 \cdot 10^{-3}$ Pa, and 0.9 Pa (end of calibration sequence)

This was done in order to realise option 3 or to check the data obtained with option 1 or 2.

For three reasons it was agreed that no bake-out should be performed with the rotors:

- 1) Bake-out is a time consuming factor and would make it impossible to have a period of one month for each laboratory.
- 2) σ_{eff} may change after a bake-out.
- 3) The rotors were transported under vacuum, so that there was no real need for a bake-out of the rotors.

Since σ_{eff} is pressure dependent for $p > 3 \cdot 10^{-2}$ Pa, which may make the comparison inaccurate, when the target pressures are not hit exactly, it was agreed that a linear fit line through the points $\sigma_{ij}(p_{stj} \approx 9 \cdot 10^{-2}$ Pa), $\sigma_{ij}(p_{stj} \approx 0.3$ Pa), and $\sigma_{ij}(p_{stj} \approx 0.9$ Pa) would be used to calculate σ_{ij} at the exact target pressures in the following manner

$$\sigma_{ij} = (\sigma_{ij})_{\text{det}} + (p_t - p_{stj}) \cdot m_i \quad (2)$$

p_t are the nominal target pressures 0.09 Pa, 0.3 Pa, 0.9 Pa, p_{stj} the generated pressures close to p_t , $(\sigma_{ij})_{\text{det}}$ the values determined by the calibration at p_{stj} , and m_i the slope of the fit line for rotor i . The uncertainty of the m_i will be neglected in the following since the p_{stj} were very close to the p_t .

At the end of this calibration procedure, for each generated p_{stj} near the respective target point and for each rotor i and for each of the calibration sequences (2 or 3) a value for σ_{ij} existed and was reported to the pilot laboratory. With the value of σ_{ij} each laboratory reported the standard uncertainty $u(p_{stj})$ of p_{stj} .

Table 4 gives an overview of how the measurements were performed. The IMG-CNR delivered calibration data in the whole range, but decided - before circulation of Draft A - to withdraw its calibration data for the three lowest target pressures $p_t \leq 3 \cdot 10^{-3}$ Pa as did CMI for all its calibration data (see Section 9).

Table 4 Overview of how measurements were performed in each laboratory. T is the mean gas temperature at which measurements were performed.

Laboratory	Both SRGs at the same time	No. of calibration sequences	Option used for offset measurement	Deviation from protocol	T in K
BNM-LNE France	yes	2	Option 2	None	295
Centro Espanol de Metrologia (CEM) Spain	yes	3	Option 3	None	294
Institute of Metals and Technology (IMT) Slovenia	yes	2	Option 3	None	298
Istituto Metrologia Gustavo Colonnetti (IMGC-CNR) Italy	yes	2	Option 1	6 calibration days due to different primary standards. Values for $p_i \leq 3 \cdot 10^{-3}$ Pa were later withdrawn.	294
National Physical Laboratory (NPL) United Kingdom	yes	3	Option 2	No point at $3 \cdot 10^{-2}$ Pa, but instead at $2 \cdot 10^{-2}$ Pa	293
Physikalisch-Technische Bundesanstalt (PTB) Germany	yes	10 (pilot lab)	Option 3	None	297
TUBITAK - Ulusal Metroloji Enstitüsü (UME) Turkey	yes	3	Option 2	No calibration at $3 \cdot 10^{-4}$ Pa	294

7. Uncertainties of reference standards

Table 5 and Figure 1 present the relative standard uncertainties due to Type B uncertainties for the various standards. Type A uncertainties will show up in the scatter of data at repeat measurements, so that it was sufficient to report the Type B uncertainties only.

It can be clearly seen that the primary standards have smaller uncertainties than those of the secondary standards due to the long-term instability of the latter. The relative uncertainties for the primary standards range typically between 0.17% and 0.3%, the secondary based standards between 0.5 % and 3.3%, with the one exception of IMT, which used an in-situ calibrated SRG as secondary standard.

Table 5 Relative standard uncertainties of generated pressures due to systematic effects (Type B) as reported by the participants.

p_i in Pa	BNM-LNE	CEM	IMGC	IMT	NPL	PTB	UME
3.00E-04	1.72E-02	3.27E-02	9.8E-03	3.30E-03	3.04E-03	2.42E-03	
9.00E-04	9.49E-03	2.33E-02	9.8E-03	2.69E-03	2.98E-03	2.42E-03	3.76E-03
3.00E-03	6.87E-03	1.90E-02	7.2E-03	2.57E-03	2.98E-03	2.42E-03	2.93E-03
9.00E-03	5.90E-03	1.78E-02	2.9E-03	2.59E-03	2.99E-03	3.15E-03	2.84E-03
3.00E-02	5.63E-03	1.80E-02	2.1E-03	2.59E-03	2.00E-03	3.15E-03	2.83E-03
9.00E-02	5.66E-03	1.78E-02	2.1E-03	2.55E-03	2.58E-03	3.04E-03	2.83E-03
3.00E-01	5.63E-03	7.00E-03	2.0E-03	2.54E-03	2.41E-03	1.67E-03	2.31E-03
9.00E-01	5.53E-03	7.00E-03	2.0E-03	2.54E-03	2.40E-03	1.67E-03	2.18E-03

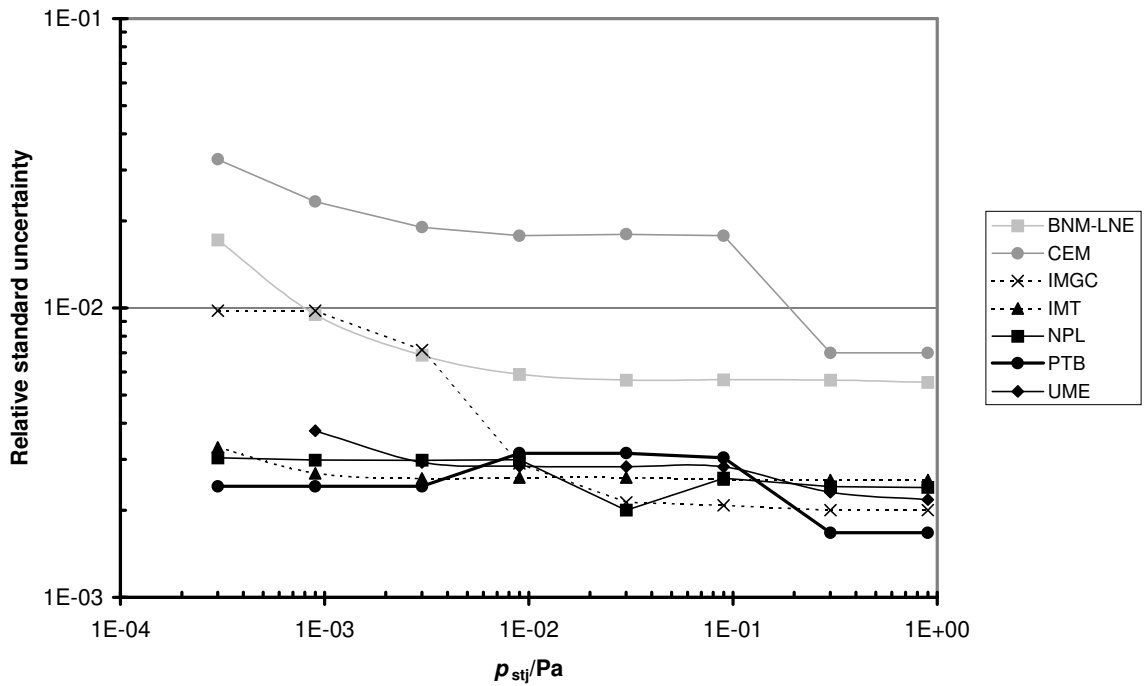


Figure 1 Relative standard uncertainties of generated pressures due to systematic (Type B) uncertainties as reported by the participants.

8. Uncertainties of reported measured values

The model of the reported value, σ_{ij} , has been formulated in Eq. (1). If we introduce

$$K_i = \sqrt{\frac{8k \cdot 296.15 \text{ K}}{\pi n} \cdot \frac{\pi d_i \rho_i}{20}}, \quad (3)$$

and

$$DCR_i \equiv \left(\frac{\dot{\omega}}{\omega} \right)_i, \quad (4)$$

and consider that the effective accommodation coefficient has been measured $n = 6$ or 9 times, σ_{ijk} , $k=1 \dots n$, then we can write,

$$\sigma_{ijk} = \sqrt{\frac{T_{jk}}{296.15}} \cdot \frac{K_i}{p_{stjk}} (DCR_{ik} - RD_{ik}(\omega)) \quad T_{jk} \text{ in K} . \quad (5)$$

We take the mean of the results of the repeated measurements to give the best estimate of the calibration constant defined in Eq. (1):

$$\sigma_{ij} = \frac{1}{n} \sum_{k=1}^n \sigma_{ijk} . \quad (6)$$

The same values for k , m , d_i , and ρ_i were used by each laboratory and the K_i were therefore fully correlated, so that in effect no uncertainty needed to be attributed to K_i (A systematic error in d_i , for example, would be calibrated into σ_{ij} in the same way in each laboratory and would not affect the result of the comparison). All type A uncertainties of values on the right hand side of Eq. (5) will contribute to the scatter of σ_{ijk} and so to the standard deviation of σ_{ij} . Therefore, since Type A uncertainties are accounted for by the standard deviation, for calculation of the overall uncertainty of σ_{ij} only the Type B uncertainties of values on the right hand side of Eq. (5) have to be evaluated for inclusion. For DCR_i there is no such uncertainty. $RD(\omega)$ is not determined at the same time as DCR_i , but before or after the measurement, and therefore has a Type B uncertainty. Also the gas temperature and the generated pressure p_{stj} will have Type B uncertainties, which are known before the measurements.

For this reason the variance in σ_{ij} is given by

$$u^2(\sigma_{ij}) = \frac{n-1}{n-3} s_{\sigma_{ij}}^2 + \left(\frac{\partial \sigma_{ij}}{\partial RD_i} \right)^2 u_{RD_i}^2 + \left(\frac{\partial \sigma_{ij}}{\partial T_j} \right)^2 u_{T_j}^2 + \left(\frac{\partial \sigma_{ij}}{\partial p_{stj}} \right)^2 u_{p_{stj}}^2 , \quad (7)$$

where $s_{\sigma_{ij}}^2$ is the square of the standard deviation of the mean of the repeat measurements σ_{ijk} and where we understand that all standard uncertainties u are due to systematic effects which do not contribute to the scatter of σ_{ij} . Since only $n = 6$ (or 9) measurements were taken with an effective degree of freedom of 5 (8), $s_{\sigma_{ij}}$ was multiplied by $\sqrt{(n-1)/(n-3)}$, i.e. 1.29 (1.15), as suggested by Kacker and Jones [11]. The last term in Eq. (7) is due to the generated pressure as discussed in Section 7, all the other terms are due to uncertainties of the measurement (transfer) standard.

The sensitivity coefficients are:

$$\left(\frac{\partial \sigma_{ij}}{\partial RD_i} \right) = -\frac{K_i}{p_{stj}} \cdot \sqrt{\frac{T_j}{296.15}} \quad T_j \text{ in K} \quad (8)$$

$$\left(\frac{\partial \sigma_{ij}}{\partial p_{stj}}\right) = -\frac{K_i}{p_{stj}^2} \cdot \sqrt{\frac{T_j}{296.15}} (DCR_i - RD_i) \quad T_j \text{ in K} \quad (9)$$

$$\left(\frac{\partial \sigma_{ij}}{\partial T_j}\right) = \frac{1}{2} \frac{K_i}{p_{stj}} \frac{1}{\sqrt{296.15}} \frac{1}{\sqrt{T_j}} (DCR_i - RD_i) \quad T_j \text{ in K} \quad (10)$$

$u(p_{stj})$ and $u(T_j)$ were reported by each laboratory, where it is assumed that $T_{jk} \approx T_j$ (constant temperature of standard during 3 repeat measurements). $u(T_j) = 0$, if another SRG was used as reference standard, since both devices are completely correlated with respect to the temperature T_j . The following effects may contribute to the uncertainty of the residual drag RD_i :

- the scatter of the measurement results
- the imprecisely known frequency dependence of the offset
- a possible short term drift of the offset value between its determination and the time of calibration
- a possible long term drift of the offset value between its determination and the time of calibration.

The latter effect was excluded by the agreed calibration procedure since it was required that a previously measured frequency dependence (Option 1 or 2) was checked during the measurements. If significant differences occurred, Option 3 had to be used to determine RD_i . There were no significant shifts (more than the scatter of the data) of the offset in the time frame for Option 3. The uncertainty due to the first three effects was considered by the evaluation of data in the pilot laboratory in the following manner: Independently of which option was used, a linear fit line through all measured $RD_i(\omega)$ was calculated (least squares). The 95% confidence limits of the predicted values were calculated. The difference between the upper and the lower confidence limit was nearly independent of ω in the measurement range. For standard uncertainty $u(RD_i(\omega))$, $\frac{1}{4}$ of the difference between the upper and the lower confidence limit was taken. With this procedure, both the scatter of $RD_i(\omega)$, the uncertainty of the frequency dependence, and possible short term shifts (within about 60 min) were included.

9. Reported results of each laboratory

Since each laboratory carried out 2 or 3 calibration sequences it was possible to check if significant changes could be observed between the σ_{ij} for the different sequences. Such a change could be important for the comparison for two reasons:

- 1) If an instability in the calibration constant of a transfer standard occurred during the calibrations in a single laboratory, it could be taken into account by normalisation. If only one SRG showed a change in value it is highly probable that such an instability was detected.
- 2) If the reference standard showed an instability, it is highly probable that both σ_{1j} and σ_{2j} would show a shift of same size in the same direction. This could help the participant to improve their standard.

If no significant change occurred, it is clear that the mean value of all data for a single rotor and single target pressure could be taken for data reduction:

$$\sigma_{ij} = \frac{1}{n} \sum_{k=1}^n \sigma_{ijk} \quad n = 6 \text{ or } 9 \quad \text{Eq. (6)}$$

Fortunately, no such changes of the calibration constant of the transfer standards were found for any of the laboratories. At the lowest target pressure there were in some cases relatively large differences between values on different days, but these could be explained by the uncertainties of *RD*. Only at UME significant changes were detected for the rotors at the target pressures of 0.3 Pa and 0.9 Pa. Since these changes, however, were not observed for all pressures for a single SRG, we treated these data in the same manner as the “normal” ones and calculated the mean. It remains the task of the laboratory to investigate this point.

The results reported by each laboratory and the corresponding uncertainties according to Eq. (7) are shown in the following tables and figures.

It was noticed that the results of two laboratories (CMI and IMGCCNR) showed a clear pressure dependence of the values of σ_{1j} and σ_{2j} in the molecular regime below 0.03 Pa, in contradiction to a priori knowledge (see Section 4). This could indicate a numerical or systematic error for the measurements in these two laboratories. For this reason both of these laboratories were informed about anomalies of data according to the CIPM guideline [12] by the pilot laboratory before finishing the Draft A report. As a result, IMGCCNR withdrew the results at the three lowest target pressures, CMI withdrew its complete data set.

Also it can be seen from the values PTB1...PTB5 that both gauges experienced a drift in their characteristics.

Table 6 The mean values σ_{ij} of the reported results for Rotor 1 for all participants and the uncertainties as calculated from Eq. (7).

p_i/Pa	PTB1	NPL	LNE	PTB2	IMT	IMGC	PTB3	CEM	PTB4	UME	PTB5
3.00E-04	1.1660	1.1647	1.1417	1.1708	1.1659		1.1585	1.1614	1.1548		1.1558
$u(\sigma_{ij})$	0.0040	0.0121	0.0422	0.0111	0.0083		0.0118	0.0504	0.0064		0.0113
9.00E-04	1.1658	1.1613	1.1576	1.1587	1.1673		1.1594	1.1592	1.1516	1.1414	1.1500
	0.0031	0.0052	0.0160	0.0049	0.0041		0.0047	0.0288	0.0034	0.0056	0.0047
3.00E-03	1.1643	1.1613	1.1591	1.1596	1.1668		1.1592	1.1566	1.1505	1.1465	1.1509
	0.0029	0.0038	0.0092	0.0030	0.0031		0.0030	0.0222	0.0028	0.0036	0.0031
9.00E-03	1.1684	1.1611	1.1607	1.1627	1.1677	1.1855	1.1582	1.1560	1.1525	1.1485	1.1539
	0.0036	0.0036	0.0070	0.0038	0.0029	0.0035	0.0036	0.0208	0.0036	0.0034	0.0037
3.00E-02	1.1650	1.1614	1.1605	1.1615	1.1672	1.1829	1.1577	1.1557	1.1514	1.1477	1.1524
	0.0037	0.0036	0.0066	0.0038	0.0029	0.0024	0.0035	0.0208	0.0036	0.0034	0.0037
9.00E-02	1.1628	1.1609	1.1597	1.1596	1.1657	1.1711	1.1558	1.1547	1.1492	1.1467	1.1502
	0.0036	0.0031	0.0067	0.0035	0.0030	0.0025	0.0036	0.0205	0.0035	0.0034	0.0035
3.00E-01	1.1573	1.1572	1.1548	1.1540	1.1602	1.1553	1.1503	1.1495	1.1436	1.1438	1.1444
	0.0020	0.0029	0.0066	0.0019	0.0030	0.0024	0.0019	0.0081	0.0019	0.0031	0.0019
9.00E-01	1.1409	1.1398	1.1390	1.1371	1.1437	1.1382	1.1344	1.1343	1.1275	1.1282	1.1283
	0.0020	0.0029	0.0063	0.0020	0.0029	0.0023	0.0019	0.0080	0.0019	0.0030	0.0019

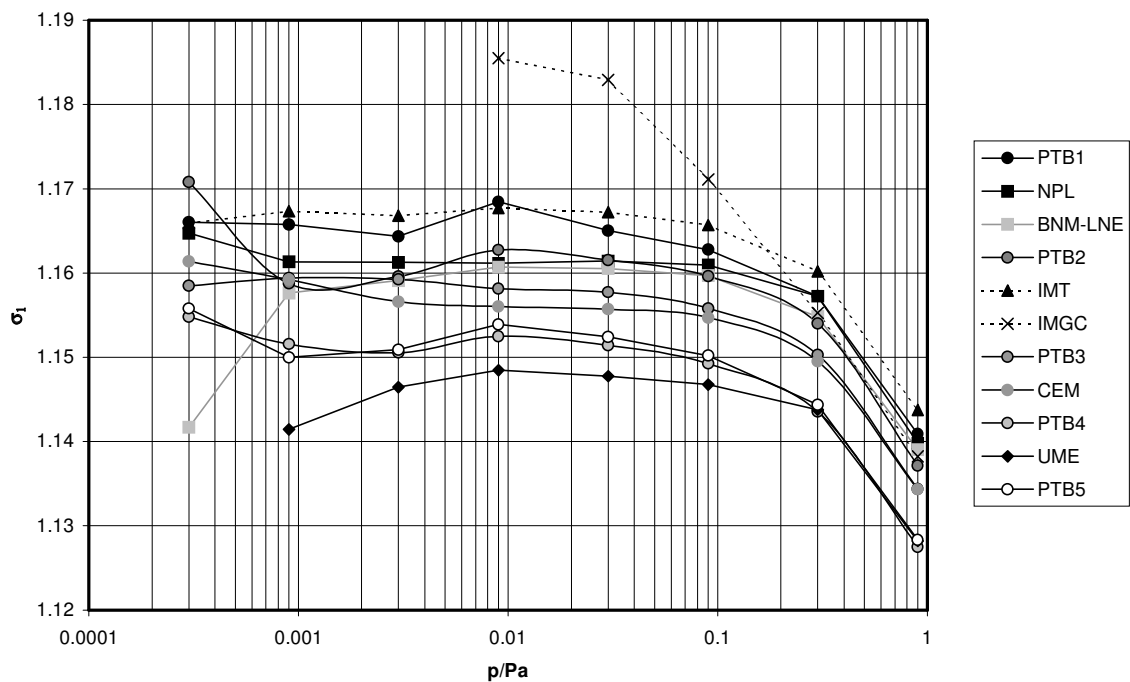


Figure 2 Graphical presentation of the results of Rotor 1 (Table 6)

Table 7 The mean values σ_{2j} of the reported results for Rotor 2 for all participants and the uncertainties as calculated from Eq. (7).

p_i/Pa	PTB1	NPL	LNE	PTB2	IMT	IMGC	PTB3	CEM	PTB4	UME	PTB5
3.00E-04	1.1369	1.1373	1.1358	1.1315	1.1333		1.1203	1.0974	1.1248		1.1144
$u(\sigma_{2j})$	0.0322	0.0039	0.0208	0.0038	0.0092		0.0068	0.0492	0.0051		0.0031
9.00E-04	1.1365	1.1345	1.1346	1.1300	1.1324		1.1215	1.1130	1.1228	1.1079	1.1144
	0.0111	0.0036	0.0109	0.0028	0.0042		0.0034	0.0279	0.0031	0.0056	0.0027
3.00E-03	1.1336	1.1330	1.1308	1.1292	1.1344		1.1215	1.1198	1.1217	1.1109	1.1144
	0.0044	0.0035	0.0083	0.0027	0.0030		0.0028	0.0215	0.0027	0.0036	0.0027
9.00E-03	1.1386	1.1324	1.1308	1.1321	1.1344	1.1666	1.1210	1.1209	1.1236	1.1128	1.1175
	0.0038	0.0035	0.0067	0.0037	0.0029	0.0070	0.0035	0.0202	0.0036	0.0034	0.0035
3.00E-02	1.1355	1.1324	1.1318	1.1309	1.1338	1.1480	1.1203	1.1214	1.1228	1.1119	1.1165
	0.0037	0.0035	0.0064	0.0037	0.0028	0.0023	0.0034	0.0202	0.0035	0.0034	0.0035
9.00E-02	1.1332	1.1321	1.1320	1.1298	1.1326	1.1365	1.1186	1.1211	1.1206	1.1110	1.1143
	0.0035	0.0031	0.0066	0.0034	0.0029	0.0025	0.0035	0.0199	0.0034	0.0034	0.0034
3.00E-01	1.1283	1.1289	1.1272	1.1246	1.1279	1.1238	1.1134	1.1168	1.1154	1.1085	1.1090
	0.0019	0.0029	0.0064	0.0020	0.0029	0.0023	0.0019	0.0079	0.0019	0.0031	0.0019
9.00E-01	1.1135	1.1131	1.1129	1.1090	1.1130	1.1084	1.0990	1.1032	1.1008	1.0946	1.0946
	0.0019	0.0028	0.0062	0.0020	0.0029	0.0023	0.0018	0.0078	0.0018	0.0030	0.0018

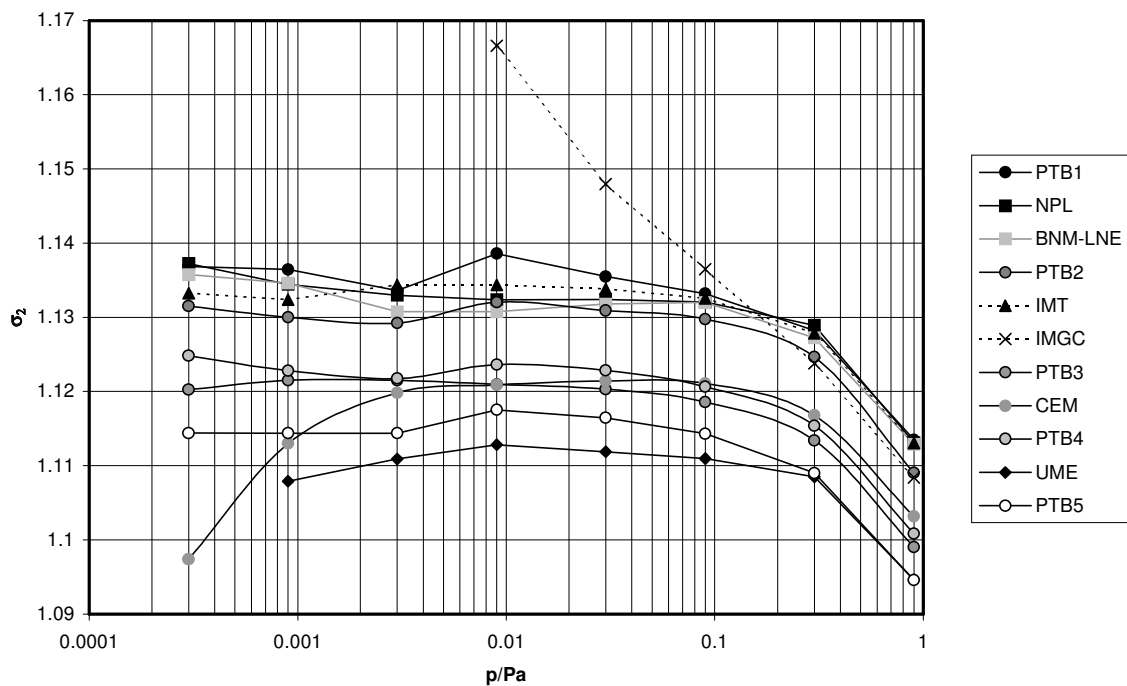


Figure 3 Graphical presentation of the results of Rotor 2 (Table 7).

10. Stability of transfer gauges

In order to monitor the stability of the calibration constant of the two rotors during the course of the comparison, the mean values of σ_1 and σ_2 between $9 \cdot 10^{-4}$ Pa and $3 \cdot 10^{-2}$ Pa of the pilot laboratory were calculated. Figure 4 shows the mean values, normalised to the first calibration of the comparison, PTB1, to illustrate the relative changes. Rotor 3 was the check standard that did not travel.

Rotor 3 has a clearly superior stability with a standard deviation of only 0.001 about the mean compared to 0.005, respectively 0.007 for Rotor 1 and Rotor 2. The stability of Rotor 3 may serve as evidence of the stability of the primary standard at the pilot laboratory. Both Rotor 1 and Rotor 2 showed the same relative downwards drift during the first loop of the comparison (between PTB1 and PTB2), but, fortunately, during the following loops at least one of the two rotors was stable with a relative change $< 0.2\%$ (see Table 8).

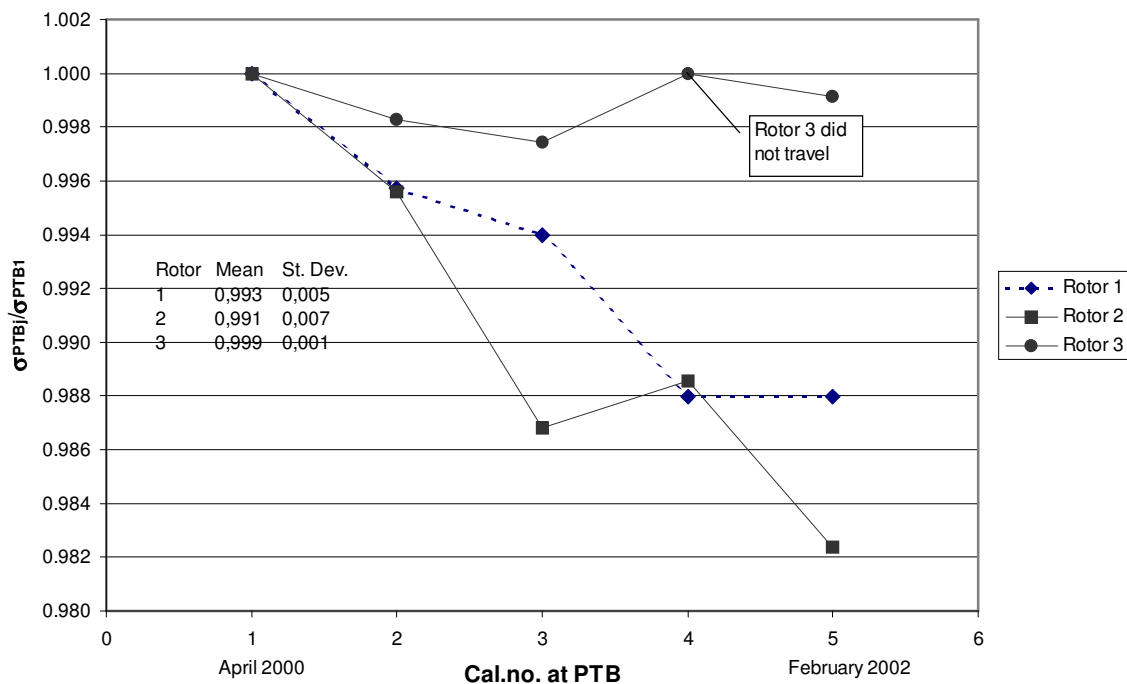


Figure 4 Normalised mean σ_i values of the pilot laboratory between $9 \cdot 10^{-4}$ Pa and $3 \cdot 10^{-2}$ Pa during the course of the comparison. Rotor 3 was used as check standard and did not travel.

To compare primary standards using unstable transfer standards, it would be ideal to calibrate the transfer standards at the same time on the different primary standards. Since this is not possible, we assumed that the mean value of the two pilot laboratory calibrations (at the

beginning and at the end of a loop) is the best approximation of coincident time to compare with the participants' values in the loop:

$$\sigma_{iPTBk,k+1} = \frac{\sigma_{iPTBk} + \sigma_{iPTBk+1}}{2} \quad k = 1 \dots 4 \quad . \quad (11)$$

Here p_{iPTBk} refers to the calibration number k at the pilot laboratory PTB ($k = 1 \dots 4$). Since σ_i is independent of pressure in the molecular regime, $\sigma_{iPTBk,k+1}$ is taken as a mean between $9 \cdot 10^{-4}$ Pa and $3 \cdot 10^{-2}$ Pa. In the transition regime ($> 3 \cdot 10^{-2}$ Pa), however, $\sigma_{iPTBk,k+1}$ is calculated for each target pressure.

In most cases the measurements during $PTBk$ and $PTBk+1$ refer to different parent populations of observations. For this reason, as an estimate of the standard uncertainty of $\sigma_{iPTBk,k+1}$ we took half of the difference of the two pilot laboratory values as it was done previously [13], [14]. This means that there is a probability of about 70% that a value within the range of values at the beginning and end of the loop would have been measured by the pilot laboratory, had it been measured coincidentally with the participant within the loop.

$$u(\sigma_{iPTBk,k+1}) = \left| \frac{\sigma_{iPTBk+1} - \sigma_{iPTBk}}{2} \right| \quad (12)$$

$\sigma_{iPTBk,k+1}$ denotes the mean of σ_{iPTBk} and $\sigma_{iPTBk+1}$ as defined in Eq. (11).

Since very similar values of σ_{iPTBk} and $\sigma_{iPTBk+1}$ could also be produced accidentally (a positive change during a transport may be cancelled out by a negative at the return transport), it was agreed that $u(\sigma_{iPTBk,k+1}) / \sigma_{iPTBk,k+1}$ shall have a cut-off of 0.15%: If the value of $u(\sigma_{iPTBk,k+1}) / \sigma_{iPTBk,k+1} < 0.15\%$ it was replaced by 0.15%.

Table 8 gives the mean values σ_{iPTB} in each of the 4 loops at the pilot laboratory and the uncertainties due to transport and/or long term instabilities of the rotors for the molecular regime. Table 9 and Table 10 give values for all other pressures. $u(\sigma_{PTB,exp})$ denotes the uncertainty as calculated by Equation (12) from the experimental data, $u(\sigma_{PTB})$ the uncertainty after introducing the cut-off mentioned above.

The Type A uncertainties contribute significantly only when the transport instability is very small, (compare the columns $\Delta/2$ and $u(\sigma_{PTB,exp})$). In a few cases the shifts of σ measured by the pilot laboratory were slightly different in the molecular regime ($\leq 3 \cdot 10^{-2}$ Pa) and the transition regime.

Table 8 Mean values of σ_{iPTB} between $9 \cdot 10^{-4}$ Pa and $3 \cdot 10^{-2}$ Pa in the molecular regime ($\leq 3 \cdot 10^{-2}$ Pa) in each of the 4 loops (e.g. PTB12 means the loop with PTB1 at the beginning and PTB2 at the end) and their respective uncertainties. $u(\sigma_{PTB,exp})$ denotes the uncertainty as calculated by Equation (12) from the experimental data, $u(\sigma_{PTB})$ the uncertainty after introducing the cut-off.

	Rotor 1			Rotor 2		
	Mean	$u(\sigma_{PTB,exp})$	$u(\sigma_{PTB})$	Mean	$u(\sigma_{PTB,exp})$	$u(\sigma_{PTB})$
PTB12	1.1633	0.0026	0.0026	1.1333	0.0027	0.0027
PTB23	1.1596	0.0010	0.0017	1.1258	0.0047	0.0047
PTB34	1.1551	0.0036	0.0036	1.1219	0.0008	0.0017
PTB45	1.1517	0.0002	0.0017	1.1192	0.0035	0.0035

Table 9 Mean values of σ_1 in the transition regime ($> 3 \cdot 10^{-2}$ Pa) in each of the 4 loops, and their respective uncertainties. $u(\sigma_{1PTB,exp})$ denotes the uncertainty as calculated by Equation (12) from the experimental data, $u(\sigma_{1PTB})$ the uncertainty after introducing the cut-off.

	0.09 Pa	$u(\sigma_{1PTB,exp})$	$u(\sigma_{1PTB})$	0.3 Pa	$u(\sigma_{1PTB,exp})$	$u(\sigma_{1PTB})$	0.9 Pa	$u(\sigma_{1PTB,exp})$	$u(\sigma_{1PTB})$
PTB12	1.1612	0.0016	0.0017	1.1556	0.0016	0.0017	1.1390	0.0019	0.0019
PTB23	1.1577	0.0019	0.0019	1.1521	0.0019	0.0019	1.1357	0.0014	0.0017
PTB34	1.1525	0.0033	0.0033	1.1469	0.0034	0.0034	1.1309	0.0034	0.0034
PTB45	1.1497	0.0005	0.0017	1.1440	0.0004	0.0017	1.1279	0.0004	0.0017

Table 10 Mean values of σ_2 in the transition regime ($> 3 \cdot 10^{-2}$ Pa) in each of the 4 loops, and their respective uncertainties. $u(\sigma_{2PTB,exp})$ denotes the uncertainty as calculated by Equation (12) from the experimental data, $u(\sigma_{2PTB})$ the uncertainty after introducing the cut-off.

	0,09 Pa	$u(\sigma_{2PTB,exp})$	$u(\sigma_{2PTB})$	0,3 Pa	$u(\sigma_{2PTB,exp})$	$u(\sigma_{2PTB})$	0,9 Pa	$u(\sigma_{2PTB,exp})$	$u(\sigma_{2PTB})$
PTB12	1.1315	0.0017	0.0017	1.1264	0.0019	0.0019	1.1113	0.0022	0.0022
PTB23	1.1242	0.0056	0.0056	1.1190	0.0056	0.0056	1.1040	0.0050	0.0050
PTB34	1.1196	0.0010	0.0017	1.1144	0.0010	0.0017	1.0999	0.0009	0.0016
PTB45	1.1175	0.0032	0.0032	1.1122	0.0032	0.0032	1.0977	0.0031	0.0031

11. Data reduction and generating a common reference value

Since one of the goals of this comparison is to generate a reference value for pressure, a pressure value had to be generated from the σ_{ij} . In each of the four loops, for each participant (except the pilot laboratory) and for each SRG i a value of indicated pressure p_{ij} for a common hypothetical target pressure p_t can be calculated with the following equation:

$$p_{ij} = p_t \cdot \frac{\sigma_{ij}}{\sigma_{iPTBk,k+1}} \quad i=1,2 \quad j=1\dots6 \quad k=1\dots4 \quad (13)$$

σ_{ij} denotes the mean accommodation coefficient according to Eq. (6) of SRG i as determined by laboratory j , $\sigma_{iPTBk,k+1}$ is the mean value obtained at the pilot laboratory in the loop under

consideration as outlined in Section 10. This normalisation ensures that systematic shifts of the accommodation coefficient of the SRGs between different loops will be cancelled out and all p_{ij} will be comparable.

The method adopted here is to use the ratios $\sigma_{ij}/\sigma_{iPTBk,k+1}$ to predict gauge readings that would be observed, when the different standards measure or generate pressures of the same value and at coincident time as the pilot laboratory in each loop. In addition, to compare results of different loops, the mean of all SRG readings taken at the pilot laboratory in the different loops are set equal to the presumably more stable pressure (see Section 10) that was realised in the pilot laboratory primary standard (see Eq. (16) below). As a result, the p_{ij} in Eq. (13) are the predicted gauge readings, when the standards realise the same value of target pressure in all loops. The difference in the predicted gauge readings is taken as an indicator of the difference between true pressures actually realised by the different standards. This latter difference between true pressures, when the standards are set to produce the same transfer gauge reading near the target pressure, is to a very good approximation (provided that the differences are small) equal to the difference in the predicted gauge readings but of opposite sign.

As was briefly mentioned at the end of Section 4 it was found by Jousten [10] that σ_{ij} may be slightly temperature dependent. The size of this effect varies from rotor to rotor and in addition is dependent on the specific surface condition of a single rotor. Relative temperature changes of $(\Delta\sigma_{eff}/\Delta T)/\sigma_{eff} = -1 \cdot 10^{-4} / \text{K}$ to $-4 \cdot 10^{-4} / \text{K}$ were found around room temperature. Table 4 shows that as a maximum the temperatures during calibrations differed by 5 K. Since the temperature dependence of σ_{eff} of the two transfer standards was not measured and also may have changed during the comparison, the only possibility to consider this effect is to add an uncertainty for the p_{ij} in Eq. (13). We assumed a calibration temperature of 296 K and a temperature dependence $(\Delta\sigma_{eff}/\Delta T)/\sigma_{eff} = -2 \cdot 10^{-4} / \text{K}$ to calculate the standard uncertainty of the temperature effect for the p_{ij} in Eq. (13):

$$u_{T\sigma}(p_{ij}) = (T_j - 296) \cdot 2 \cdot 10^{-4} p_{ij} \quad T_j \text{ in K.} \quad (14)$$

It should be emphasised that this uncertainty contribution is not in any sense related to the quality of the standard or the quality of the measurements, but only due to an incomplete specification of the protocol. At a maximum, however, this uncertainty is $6 \cdot 10^{-4} p_{ij}$ and therefore small compared to the standard uncertainties of the generated pressures (see Table 5).

Since p_t is simply a numerical value without uncertainty, the uncertainty of p_{ij} is calculated from the following equation (except for the pilot laboratory):

$$u(p_{ij}) = p_{ij} \sqrt{\left(\frac{u(\sigma_{ij})}{\sigma_{ij}}\right)^2 + \left(\frac{u(\sigma_{iPTBk,k+1})}{\sigma_{iPTBk,k+1}}\right)^2 + \left(\frac{u_{T\sigma}(p_{ij})}{p_{ij}}\right)^2} \quad (15)$$

$u(\sigma_{ij})$ was given in Eq. (7), $u(\sigma_{iPTBk,k+1})$ in Eq. (12), and $u_{T\sigma}(p_{ij})$ in Eq. (14). The input quantities in Eq. (13) are not correlated.

In the case of the pilot laboratory there are two calibrations in each loop. For this reason Eq. (13) modifies to:

$$p_{iPTBk,k+1} = p_t \cdot \frac{\sigma_{iPTBk} + \sigma_{iPTBk+1}}{2 \sigma_{iPTBk,k+1}} \quad i=1,2 \quad k=1\dots 4, \quad (16)$$

where p_{iPTBk} denotes again the calibration number k at the pilot laboratory PTB ($k = 1\dots 4$). In the molecular regime $\sigma_{iPTBk,k+1}$ is taken as a mean between $9 \cdot 10^{-4}$ Pa and $3 \cdot 10^{-2}$ Pa and therefore $p_{iPTBk,k+1}$ will be generally slightly different from p_t , in the transition regime ($> 3 \cdot 10^{-2}$ Pa) however, it will be identical to p_t .

In analogy to Eq. (15) we have

$$u(p_{iPTBk,k+1}) = p_{iPTBk,k+1} \sqrt{\left(\frac{u\left(\frac{\sigma_{iPTBk} + \sigma_{iPTBk+1}}{2}\right)}{\frac{\sigma_{iPTBk} + \sigma_{iPTBk+1}}{2}}\right)^2 + \left(\frac{u(\sigma_{iPTBk,k+1})}{\sigma_{iPTBk,k+1}}\right)^2 + \left(\frac{u_{T\sigma}(p_{iPTBk,k+1})}{p_{iPTBk,k+1}}\right)^2} \quad (17)$$

$i=1,2 \quad k=1\dots 4$

with

$$u^2\left(\frac{\sigma_{iPTBk} + \sigma_{iPTBk+1}}{2}\right) = \left(\frac{\partial \sigma_{ij}}{\partial p_{stj}}\right)^2 u_{p_{stj}}^2 + \quad (18)$$

$$0,25 \left[s_{\sigma_{iPTBk}}^2 + \left(\frac{\partial \sigma_{ij}}{\partial RD_i}\right)^2 u_{RD_{iPTBk}}^2 + \left(\frac{\partial \sigma_{ij}}{\partial T_j}\right)^2 u_{T_{PTBk}}^2 \right] +$$

$$0,25 \left[s_{\sigma_{iPTBk+1}}^2 + \left(\frac{\partial \sigma_{ij}}{\partial RD_i}\right)^2 u_{RD_{iPTBk+1}}^2 + \left(\frac{\partial \sigma_{ij}}{\partial T_j}\right)^2 u_{T_{PTBk+1}}^2 \right] \quad i=1,2 \quad k=1\dots 4$$

The first term on the right hand side describes the Type B variance of the primary standard (σ_{iPTBk} and $\sigma_{iPTBk+1}$ are correlated by p_{stPTB}) the first square bracket the Type A and Type B variances during PTB k , the second during PTB $k+1$ (see Eq. (7)).

In order to produce a single value for the pilot laboratory as for all other participants, in this context we introduce a combined variance that describes all variances but the one of p_{stPTB} for the pilot laboratory in a given loop $k, k+1$:

$$u_{iPTBk,k+1}^2 \equiv u_A^2(p_{iPTBk,k+1}) = p_{iPTBk,k+1}^2 \cdot \quad (19)$$

$$\left\{ \begin{array}{l} 0,25 \left[s_{\sigma_{iPTBk}}^2 + \left(\frac{\partial \sigma_{ij}}{\partial RD_i} \right)^2 u_{RD_{iPTBk}}^2 + \left(\frac{\partial \sigma_{ij}}{\partial T_j} \right)^2 u_{T_{PTBk}}^2 \right] / \left(\frac{\sigma_{iPTBk} + \sigma_{iPTBk+1}}{2} \right) + \\ 0,25 \left[s_{\sigma_{iPTBk+1}}^2 + \left(\frac{\partial \sigma_{ij}}{\partial RD_i} \right)^2 u_{RD_{iPTBk+1}}^2 + \left(\frac{\partial \sigma_{ij}}{\partial T_j} \right)^2 u_{T_{PTBk+1}}^2 \right] / \left(\frac{\sigma_{iPTBk} + \sigma_{iPTBk+1}}{2} \right) + \\ \left(\frac{u(\sigma_{iPTBk,k+1})}{\sigma_{iPTBk,k+1}} \right)^2 \end{array} \right.$$

$i = 1,2 \quad k = 1 \dots 4$

The first term on the right hand side describes the Type A and Type B variances during PTB k , the second during PTB $k+1$ (see Eq. (7)), the third term the uncertainty of the pilot laboratory reference value within the loop $k, k+1$ due to transport instability of the transfer standard (Eq. (12)). All input quantities for $p_{iPTBk,k+1}$ with the uncertainties on the right hand side of Eq. (19) may be considered uncorrelated.

The single value for the pilot laboratory is calculated by the mean of all $p_{iPTBk,k+1}$

$$p_{iPTB} = \frac{p_{iPTB12} + p_{iPTB23} + p_{iPTB34} + p_{iPTB45}}{4}, \quad (20)$$

the variance of which is given by

$$u^2(p_{iPTB}) = p_{iPTB}^2 \frac{\left(\frac{\partial \sigma_{ij}}{\partial p_{stj}} \right)^2 u_{p_{stj}}^2}{\bar{\sigma}_{iPTB}^2} + u_{T\sigma}^2(p_{iPTB}) + \frac{1}{16} \sum_{k=1}^4 u_{iPTBk,k+1}^2, \quad (21)$$

where the $u_{iPTBk,k+1}$ were defined in Eq. (19) and $\bar{\sigma}_{iPTB}$ is the mean of all σ_{iPTBk} as a reasonable approximation. All $p_{iPTBk,k+1}$ are correlated via the input quantity p_{stPTB} the variance of which is the first term on the right hand side of Eq. (21). The second term describes the uncertainty contribution due to the temperature dependence of σ_{eff} as described before Eq. (14). For u_T it is conservatively assumed that $p_{1PTBk,k+1}$ and $p_{2PTBk,k+1}$, and respectively $\sigma_{1PTBk,k+1}$ and $\sigma_{2PTBk,k+1}$, are correlated by their temperature dependence of σ_{eff} .

Having done this, for each laboratory and for each target point there are two values: p_{1j} and p_{2j} . Generally, these values will be slightly different. p_{1j} and p_{2j} are correlated, because the same standard j was used to determine σ_{1j} and σ_{2j} . In the Appendix it is outlined that the

easiest way to consider this correlation is to omit $u(p_{stj})$ in Eq. (7) for the determination of $u(\sigma_{ij})$ in Eq. (15), respectively to omit the first term on the right-hand side of Eq. (21) in the case of the pilot laboratory. The respective value is called u' . The weighted mean of p_{1j} and p_{2j} is then calculated for each participant and for each target point by

$$p_j = \frac{p_{1j} / u'(p_{1j})^2 + p_{2j} / u'(p_{2j})^2}{1/u'(p_{1j})^2 + 1/u'(p_{2j})^2}. \quad (22)$$

It is preferable to use the weighted mean, because this ensures that the SRG with the higher stability and/or less scatter in the results gets more weight than the other.

The standard uncertainty of p_j is

$$u(p_j) = \sqrt{\left(\frac{u(p_{stj})}{p_{stj}}\right)^2 p_j^2 + (u_{T\sigma}(p_j))^2 + \left(\frac{1}{u'(p_{1j})^2} + \frac{1}{u'(p_{2j})^2}\right)^{-1}}. \quad (23)$$

The first term under the square root describes the influence of the uncertainty of the pressure p_{stj} generated by standard j that correlates to both p_{1j} and p_{2j} , the second term the uncertainty contribution due to the temperature dependence of σ_{eff} as described before Eq. (14), and the third term in the bracket all other influences, which are due to the rotor instability, offset determination RD , temperature and scatter of data. Also for $u_{T\sigma}$ it is conservatively assumed that p_{1j} and p_{2j} , and respectively σ_{1j} and σ_{2j} , are correlated by their temperature dependence of σ_{eff} .

With the mean value p_j of the two SRGs one value with a corresponding standard uncertainty exists for each laboratory and for each target pressure.

To calculate a reference value, there are at least two approaches for inclusion of laboratories. One is to choose from general criteria, the other is a strict numerical criterion [15]. Possible general criteria are listed in the following table.

Table 11 General criteria for inclusion of laboratories to calculate a reference value

Criteria	Note	Fulfilled by
1. Independent Standard	No correlation of results between participants	BNM, IMT, IMG-CNR, NPL, PTB, UME
2. Primary standard (no direct comparison of transfer standard with secondary standard)	Highest metrological quality	IMG-CNR, NPL, PTB, UME ($\geq 9 \cdot 10^{-4}$ Pa)
3. In BIPM-CMC tables listed	Established laboratory with a checked standard and with checked uncertainties	BNM, CEM, IMG-CNR, NPL, PTB, UME

Criterion 1 is a requirement that has to be fulfilled absolutely. It was agreed among the participants that at least one more criterion has to be fulfilled by a laboratory to be included for the determination of the reference value. In this way, BNM-LNE, IMGC-CNR, NPL, PTB and UME were considered, UME only for pressures $\geq 9 \cdot 10^{-4}$ Pa. IMGC-CNR did withdraw its results up to $\leq 3 \cdot 10^{-3}$ Pa, and it is apparent from Section 9 that for the target pressure range $p_t = 3 \cdot 10^{-3}$ Pa... $9 \cdot 10^{-2}$ Pa there is a systematic problem in the IMGC-CNR results, because σ_{iIMGC} should be nearly pressure independent, as it is known a priori. For this reason the results by IMGC-CNR in this pressure range were excluded.

As a result of this discussion, Table 12 lists the laboratories which value can be included for the calculation of the reference pressure p_{EUR} .

Table 12 Laboratories which values can be included for the calculation of the reference pressure

p_t in Pa	Laboratories included
$3 \cdot 10^{-4}$	BNM-LNE, NPL, PTB
$9 \cdot 10^{-4}$	BNM-LNE, NPL, PTB, UME
$3 \cdot 10^{-3}$	BNM-LNE, NPL, PTB, UME
$9 \cdot 10^{-3}$	BNM-LNE, NPL, PTB, UME
$9 \cdot 10^{-2}$	BNM-LNE, NPL, PTB, UME
$3 \cdot 10^{-2}$	BNM-LNE, NPL, PTB, UME
0,3	BNM-LNE, IMGC-CNR, NPL, PTB, UME
0,9	BNM-LNE, IMGC-CNR, NPL, PTB, UME

The more technical approach by Cox [15] requires also the independency of the standards and passing the so called consistency test of the reference value. This consistency check was carried out here for a variety of laboratories at various pressures. Most consistency tests failed, if other than the laboratories in Table 12 were included, so that the two approaches are consistent and in agreement.

After Cox [15] the key comparison reference value was calculated as weighted mean for each target pressure by

$$p_{EUR} = \frac{\sum_{j=1}^N \frac{p_j}{u^2(p_j)}}{\sum_{j=1}^N \frac{1}{u^2(p_j)}} \quad (24)$$

where N is the number of laboratories included for the reference value (see Table 12). The standard deviation of p_{EUR} was determined by

$$u(p_{EUR}) = \sqrt{\frac{1}{\sum_{j=1}^N \frac{1}{u^2(p_j)}}}. \quad (25)$$

It makes sense to make p_{EUR} identical to p_t as it was done in the key comparison CCM.P-K4 [14]. For this we introduce the scaling factor f_c which is defined

$$f_c = \frac{p_t}{\frac{1}{N} \sum_{j=1}^N p_j}, \quad (26)$$

where N is again the number of participants that contribute to the reference value p_{EUR} . From this:

$$\begin{aligned} p_{jc} &= f_c p_j \quad \text{and} \\ p_{eur} &= f_c p_{EUR} \equiv p_t \end{aligned} \quad (27)$$

We consider f_c (≈ 1) as a pure numerical scaling factor with no uncertainty, since it simply sets equal the SRG readings in all loops to the mean pressure value of all participants contributing to the reference value instead to the value of the pilot laboratory (PTB) only (see Eqs. (13) and (16)). Since $0.998 \leq f_c \leq 1.002$, it is justified to set $u(p_{jc}) = u(p_j)$ and $u(p_{eur}) = u(p_{EUR})$. Table 13 shows the values p_{jc} and p_{eur} for each target pressure and the standard uncertainties.

Table 13 The reference pressure p_{eur} calculated from Eq. (24) and (27) and the respective p_{jc} of the participants calculated from Eq. (22) and (27) and the standard uncertainties calculated from Eq. (25) respectively (23). All units in Pa.

p_t in Pa	NPL	LNE	IMT	IMGC	GEM	UME	PTB mean	p_{eur}
3.0E-04	3.004E-04	3.000E-04	3.012E-04		2.971E-04		2.997E-04	3.000E-04
$u(p_{jc})$	1.3E-06	5.5E-06	1.8E-06		1.2E-05		1.1E-06	8.1E-07
9.0E-04	9.002E-04	9.008E-04	9.058E-04		8.981E-04	8.915E-04	8.998E-04	9.000E-04
	3.4E-06	8.9E-06	3.3E-06		2.2E-05	4.1E-06	2.5E-06	1.8E-06
3.0E-03	3.003E-03	2.998E-03	3.025E-03		3.004E-03	2.990E-03	3.004E-03	3.000E-03
	1.1E-05	2.3E-05	9.0E-06		5.8E-05	1.0E-05	7.8E-06	5.2E-06
9.0E-03	9.000E-03	8.992E-03	9.075E-03	9.224E-03	9.008E-03	8.981E-03	9.021E-03	9.000E-03
	3.2E-05	5.5E-05	2.6E-05	3.0E-05	1.6E-04	2.9E-05	2.9E-05	1.6E-05
3.0E-02	3.002E-02	3.000E-02	3.025E-02	3.066E-02	3.005E-02	2.993E-02	3.005E-02	3.000E-02
	1.1E-04	1.8E-04	8.8E-05	7.5E-05	5.4E-04	9.6E-05	9.8E-05	5.5E-05
9.0E-02	9.010E-02	9.003E-02	9.071E-02	9.112E-02	9.022E-02	8.978E-02	9.009E-02	9.000E-02
	2.6E-04	5.2E-04	2.7E-04	2.4E-04	1.6E-03	2.9E-04	2.9E-04	1.5E-04
3.0E-01	3.003E-01	2.998E-01	3.019E-01	3.006E-01	3.004E-01	2.994E-01	2.998E-01	3.000E-01
	8.4E-04	1.7E-03	9.1E-04	7.9E-04	2.2E-03	8.7E-04	5.6E-04	3.6E-04
9.0E-01	9.004E-01	9.000E-01	9.059E-01	9.016E-01	9.021E-01	8.988E-01	8.994E-01	9.000E-01
	2.6E-03	5.1E-03	2.7E-03	2.3E-03	6.4E-03	2.5E-03	1.7E-03	1.1E-03

For illustration of the differences between values of the laboratories and the reference value, it is convenient to calculate the relative difference according to

$$d_j = \frac{p_{jc}}{p_{eur}} - 1. \quad (28)$$

Figure 5 to Figure 8 illustrate the d_j with different scales on the ordinate. In Figure 7 and Figure 8 the values on the pressure axis were shifted for better visibility, but it is understood that the closely packed data points belong to the same target pressure point.

For the laboratories j that contributed to the reference value, the uncertainty is [15]

$$U(d_j) = 2 \sqrt{\left(\frac{u(p_{jc})}{p_{jc}}\right)^2 - \left(\frac{u(p_{eur})}{p_{eur}}\right)^2}, \quad (29)$$

while for the other participants j

$$U(d_j) = 2 \sqrt{\left(\frac{u(p_{jc})}{p_{jc}}\right)^2 + \left(\frac{u(p_{eur})}{p_{eur}}\right)^2}. \quad (30)$$

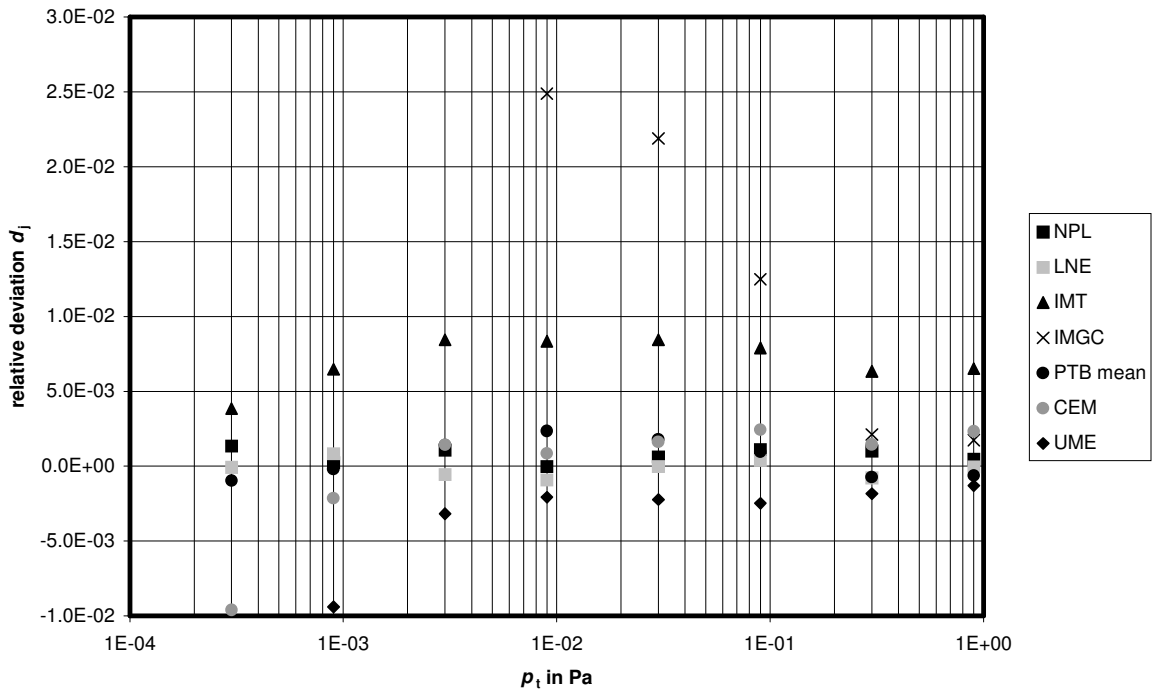


Figure 5 The d_j according to Eq. (28) for all participants. For better visibility, no uncertainty bars are shown. The uncertainties can be taken from Table 14 or Figure 7.

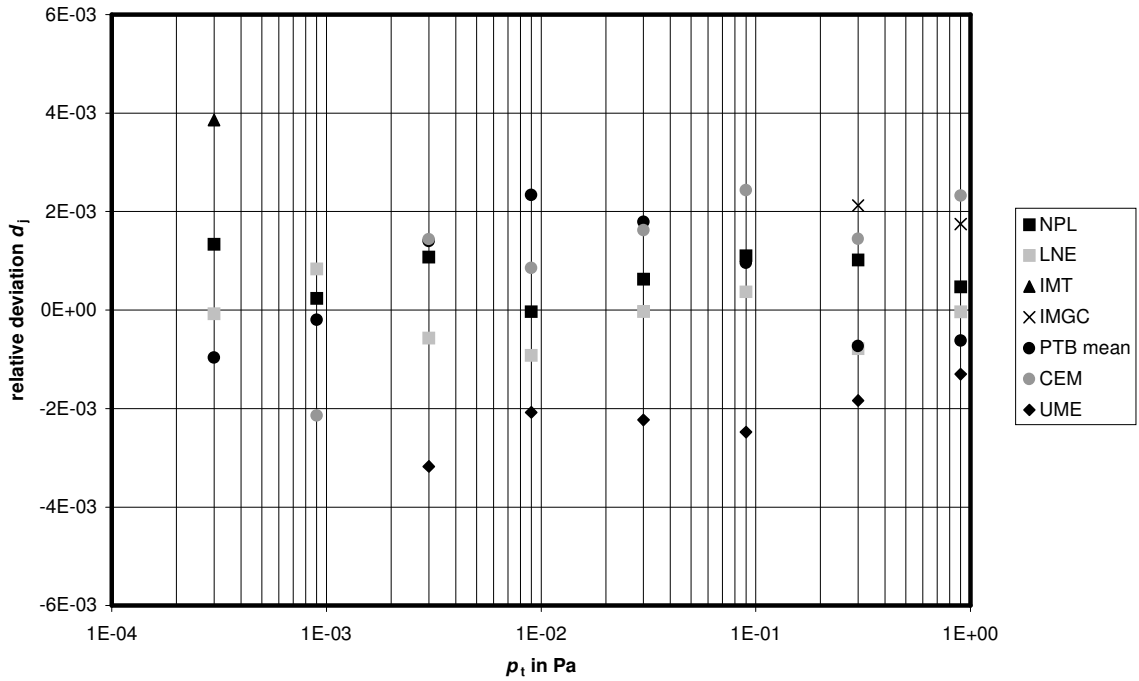


Figure 6 The d_j according to Eq. (28) near the reference value. Values $> 0.6\%$ and $< -0.6\%$ relative deviation from the reference value are not shown. For better visibility, no uncertainty bars are shown. The uncertainties can be taken from Table 14 or Figure 7.

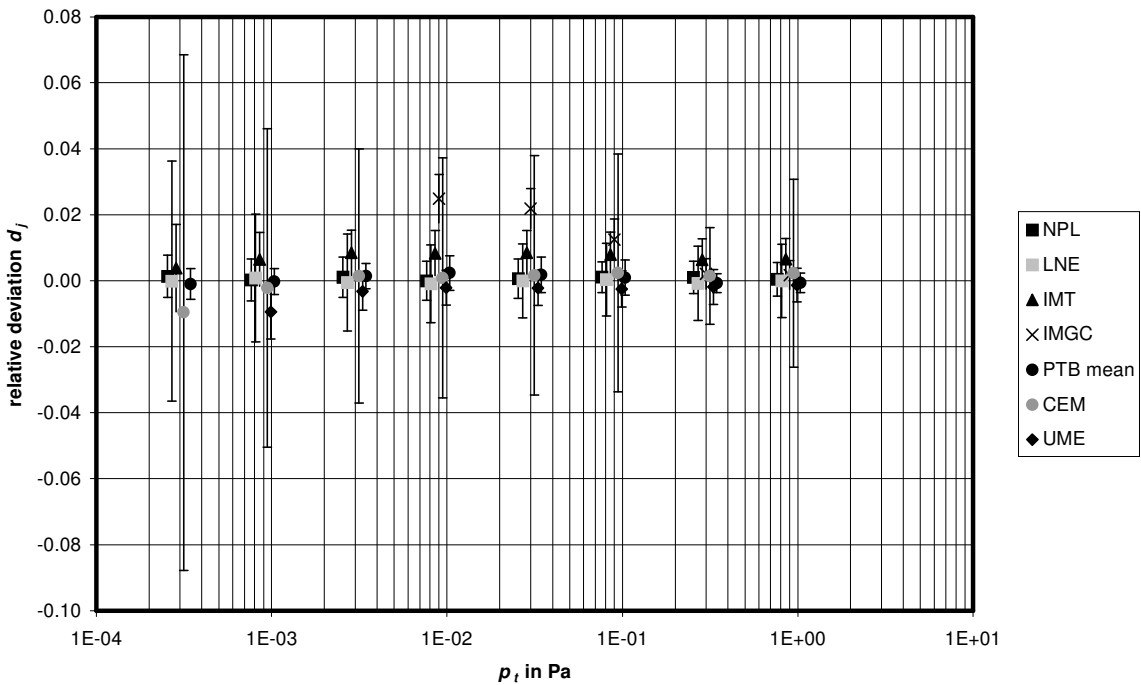


Figure 7 The d_j according to Eq. (28) for all participants. Uncertainty bars according to Eqs (29) and (30) are shown. For better visibility, the values on the pressure axis were shifted.

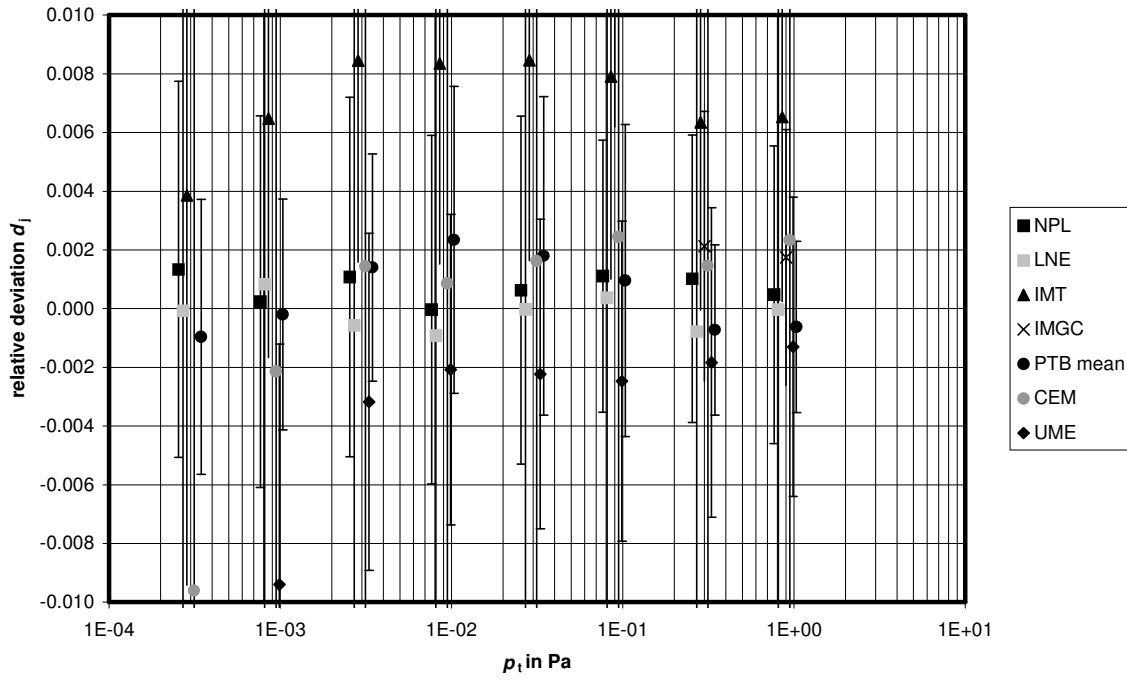


Figure 8 The d_j according to Eq. (28) near the reference value. Uncertainty bars are shown, but exceed the scale in many cases. For their complete range, see Figure 7. For better visibility, the values on the pressure axis were shifted.

To determine the degree of equivalence of each participant with the reference value, the value

$$E_j = \frac{d_j}{U(d_j)} \quad (31)$$

is calculated and one normally assumes equivalence with the reference value, if $|E_j| \leq 1$. Table 14 shows the values d_j and $U(d_j)$ for all participants, Table 15 the degrees of equivalence E_j .

Non-equivalence can be seen for some target pressures for IMT, IMGC-CNR, and for the lowest pressure in the case of UME.

Table 14 d_j (Eq. (28)) and $U(d_j)$ according to Eqs (29) and (30) for all participants.

p_l/Pa	NPL	LNE	IMT	IMGC	CEM	UME	PTB
3.0E-04	0.0013	-0.0001	0.0039		-0.0096		-0.0010
$U(d_j)$	0.0065	0.036	0.013		0.078		0.0047
9.0E-04	0.0002	0.0008	0.0065		-0.0021	-0.0094	-0.0002
	0.0064	0.019	0.0082		0.048	0.0082	0.0039
3.0E-03	0.0011	-0.0006	0.0084		0.0014	-0.0032	0.0014
	0.0062	0.015	0.0069		0.039	0.0058	0.0039
9.0E-03	0.0000	-0.0009	0.0083	0.0249	0.0008	-0.0021	0.0023
	0.0060	0.012	0.0069	0.0074	0.036	0.0053	0.0052
3.0E-02	0.0006	0.0000	0.0085	0.0219	0.0016	-0.0022	0.0018
	0.0060	0.011	0.0069	0.0061	0.036	0.0053	0.0054
9.0E-02	0.0011	0.0004	0.0079	0.0125	0.0024	-0.0025	0.0010
	0.0047	0.011	0.0070	0.0064	0.036	0.0055	0.0054
3.0E-01	0.0010	-0.0008	0.0064	0.0021	0.0015	-0.0018	-0.0007
	0.0050	0.011	0.0065	0.0047	0.015	0.0053	0.0029
9.0E-01	0.0005	0.0000	0.0065	0.0018	0.0023	-0.0013	-0.0006
	0.0052	0.011	0.0063	0.0044	0.014	0.0051	0.0029

Table 15 Degrees of equivalence E_j of the participants with this Euromet reference value as calculated from Eq. (31). A high value of E_j can be caused by a small value of $U(d_j)$ or a large value of d_j , a low value of E_j vice versa. For this reason in the last line the mean of the absolute value of the relative deviation d_j from the reference value for all 8 target pressures is also listed. Non-equivalence (if values rounded to 2 digits) is shown by slanted numbers.

p_l in Pa	NPL	LNE	IMT	IMGC	CEM	UME	PTB
3.0E-04	0.21	0.00	0.29		-0.12		-0.20
9.0E-04	0.04	0.04	0.79		-0.04	-1.14	-0.05
3.0E-03	0.17	-0.04	1.22		0.04	-0.55	0.36
9.0E-03	-0.01	-0.08	1.21	3.35	0.02	-0.39	0.45
3.0E-02	0.10	0.00	1.23	3.59	0.04	-0.42	0.33
9.0E-02	0.24	0.04	1.14	1.96	0.07	-0.45	0.18
3.0E-01	0.20	-0.07	0.98	0.46	0.10	-0.34	-0.25
9.0E-01	0.09	0.00	1.03	0.40	0.16	-0.25	-0.21
$\frac{\sum_{l=1}^8 d_j(p_l) }{8}$	7.4E-04	4.5E-04	7.0E-03	2.1E-02	2.7E-03	2.8E-03	1.1E-03

12. Link to key comparison CCM.P-K4

Table 16 lists the ratio $\frac{p_j}{p_{ref}}$ of the generated pressure to the reference value for CCM.P-K4

and this comparison for those laboratories (IMGC-CNR, NPL and PTB) that took part in both comparisons. It should be mentioned that PTB used different primary standards in the CCM

comparison and this comparison, but the two primary standards involved were compared at the beginning and the end of this Euromet comparison by use of the two transfer standards. No difference of the calibration results of the transfer gauges were found within the Type A uncertainties of the measurements, which gives sufficient confidence in the assumption that the two primary standards do agree.

Table 16 Relative values $\frac{p_j}{p_{ref}}$ of p_j to the reference value p_{ref} for key comparison CCM.P-K4 ($p_{ref} = p_{CCM} = 1$ Pa) and this comparison ($p_{ref} = p_{eur} = 0,9$ Pa). Standard uncertainties are also shown.

	IMGC		NPL		PTB	
CCM.P-K4	1.0023	± 0.0031	1.0013	± 0.0031	1.0002	± 0.0015
EUROMET.M.P-K1.b	1.0016	± 0.0025	1.0004	± 0.0028	0.9993	± 0.0019

Looking at Table 16 there is clear evidence that there is a high correlation between the differences $\frac{p_j}{p_{ref}} - \frac{p_i}{p_{ref}}$ for each pair of NMI j, i ($j \neq i$) between the CCM.P-K4 and the

EUROMET.M.P-K1.b and also for the differences $\frac{p_j}{p_{CCM}} - \frac{p_j}{p_{eur}}$. This means that the relative

positions of the p_j of the primary standards among the three NMI were the same in the two key comparisons. This is further detailed in Table 17. It has to be mentioned, however, that

the Type A uncertainties of $\frac{p_j}{p_i}$ are typically of the order of 0.002 (it is assumed that the generated pressures are correlated in the two comparisons), so that a mere coincidence of these observed correlations cannot be excluded.

Table 17 Ratios $\frac{p_j}{p_i}$ of each pair of NMI in the two comparisons. Uncertainties of the ratios due to random effects are typically 0.002.

	p_{IMGC}/p_{NPL}	p_{IMGC}/p_{PTB}	p_{NPL}/p_{PTB}
CCM.P-K4	1.0010	1.0021	1.0011
EUROMET.M.P-K1.b	1.0012	1.0023	1.0011

At least two approaches to link results of CIPM and RMO comparisons have been published recently by Elster et al. [17] and, Delahaye and Witt [18]. Another approach similar to [17] is suggested here:

Let

$$X = \frac{\sum_{i=1}^n (X_i / u^2(x_i))}{\sum_{i=1}^n (1/u^2(x_i))} \quad (32)$$

be the weighted mean (reference value) of all the quantities related to a CIPM comparison with $i = 1, \dots, n$ participants and

$$Y = \frac{\sum_{k=1}^m (Y_k / u^2(y_k))}{\sum_{k=1}^m (1/u^2(y_k))} \quad (33)$$

be the weighted mean (reference value) of all the quantities related to the RMO comparison to be linked to the CIPM comparison with $k = 1, \dots, m$ participants. Let us assume that $l = 1, \dots, L$ laboratories have participated in both the CIPM and the RMO comparison.

Then we define

$$\bar{X} = \frac{\sum_{l=1}^L (X_l / u^2(x_l))}{\sum_{l=1}^L (1/u^2(x_l))} \quad (34)$$

as the weighted mean of the quantities in the CIPM comparison of the linking laboratories only and

$$\bar{Y} = \frac{\sum_{l=1}^L (Y_l / u^2(y_l))}{\sum_{l=1}^L (1/u^2(y_l))} \quad (35)$$

as the weighted mean of the quantities in the RMO comparison of the linking laboratories.

The Y_k shall be transformed to Z_k , so that a direct comparison of all RMO participants with the reference value in CIPM comparison and the evaluation of the degree of equivalence is possible. It is suggested that

$$Z_k = RY_k, \quad (36)$$

which defines

$$\bar{Z} = R\bar{Y}. \quad (37)$$

\bar{Z} is the mean value of the linking laboratories in the RMO comparison after transformation. The transformation shall be carried out in such a manner that

$$\frac{\bar{X} - X}{X} = \frac{\bar{Z} - X}{X}. \quad (38)$$

This equation means that the mean of the relative deviations of the linking laboratories to the CIPM reference value after transformation from the RMO comparison (right hand side of Eq. (38)) is the same as for the CIPM comparison (left hand side of Eq. (38)). To carry out the transformation in such a manner that (38) is fulfilled is reasonable, if stability of the standards involved in both comparisons is assumed.

It follows from Eqs. (37) and (38) that

$$R = \frac{\bar{X}}{\bar{Y}}. \quad (39)$$

For this comparison, under the assumption that the primary standards of the three NMI remained stable in between the comparisons and realised the scale in the same manner for the two closest matched target pressures (0.9 Pa and 1 Pa) of the two comparisons, a link to the CCM comparison can be made in the way described above:

Let us call

$$p_{ccm,link} = \frac{\sum_{l=1}^3 (p_{CCM,l} / u^2(p_{ccm,l}))}{\sum_{l=1}^3 (1/u^2(p_{ccm,l}))} \quad (40)$$

the weighted mean of the generated pressures of the three linking NMIs (IMGC-CNR, NPL, and PTB) of the CCM comparison (corresponding to the quantity \bar{X}) and

$$p_{eur,link} = \frac{\sum_{l=1}^3 (p_{eur,l} / u^2(p_{eur,l}))}{\sum_{l=1}^3 (1/u^2(p_{eur,l}))} \quad (41)$$

the weighted means of the generated pressures of the three linking NMIs (IMGC-CNR, NPL, and PTB) of this Euromet comparison (corresponding to the quantity \bar{Y}). Then R is estimated by

$$r = \frac{p_{CCM,link}}{p_{eur,link}} = 1.11158. \quad (42)$$

Since the target pressures were different by the ratio $1\text{Pa}/0.9\text{ Pa} = 1.11111$ the value of r in Eq. (42) means that the two reference values are relatively shifted by $1.11158/1.11111=1.0004$. This relative shift of 0.0004 is so small compared with the relative standard uncertainties of $u(p_{\text{eur}})/p_{\text{eur}}=0.0011$ at $p_{\text{eur}}=0.9\text{ Pa}$ and $u(p_{\text{CCM}})/p_{\text{CCM}}=0.0008$ at $p_{\text{CCM}}=1\text{ Pa}$ (p_{eur} and p_{CCM} being the respective reference values), that it can be considered as insignificant. Because of this fact it is not necessary to make a transformation of all the data at 0.9 Pa of the participants of the Euromet comparison to the CCM key comparison as suggested by Eq. (36).

In consequence, the insignificantly small relative shift means two things: The two reference values of the CCM.P-K4 and EUROMET.M.P-K1.b are in agreement at the one overlapping point at 0.9 Pa and the degrees of equivalence with the reference value after transformation to the CCM.P-K4 would be very much the same as for the EUROMET.M.P-K1.b reference value.

13. Discussion and conclusions

In the present comparison, the degrees of equivalence of 7 NMIs within EUROMET for the pressure scale from $3 \cdot 10^{-4}\text{ Pa}$ up to 0.9 Pa were evaluated. One of the results was that 4 of the 7 NMIs, namely CEM, LNE, NPL, and PTB were equivalent with the EUROMET reference pressure for the whole range. The results for UME showed non-equivalence at $9 \cdot 10^{-4}\text{ Pa}$ only. In addition, all NMIs can be considered equivalent for the pressure values 0.3 Pa and 0.9 Pa, when the degree of equivalence is rounded to 2 digits.

Below 0.3 Pa, the IMGCC-CNR results showed significant deviations from the EUROMET reference value. Apparently, the continuous expansion system of IMGCC-CNR which was used below 0.3 Pa had a severe problem and cannot be considered as equivalent.

The IMT results showed non-equivalence between $3 \cdot 10^{-3}\text{ Pa}$ and $9 \cdot 10^{-2}\text{ Pa}$, but equivalence for all other pressures. As the reason for the non-equivalence IMT identified an underestimation of its uncertainties and increased them as a consequence of this comparison.

All static expansion systems as primary standards were fully in agreement within the significance of this comparison, with one exception, i.e. UME at $9 \cdot 10^{-4}\text{ Pa}$. It is interesting to see that the LNE, using a very different approach to calibrate its secondary standard that is independent of any other NMI by its method, showed very small deviations from the reference value over the whole range. Though also CEM showed very low E_n values (a high degree of equivalence), these were mainly caused by relatively high uncertainties of the

standard pressure (see Figure 1). CEM conservatively used either the uncertainties that were delivered for the CMC tables or as calculated from a more recent calibration certificate of their SRG reference standard whichever were larger. For this reason there is a step in the uncertainty values between 0.09 Pa and 0.3 Pa (see Table 5 and Figure 1). If the uncertainties as calculated from the more recent calibration certificate of their reference standard had been used, the uncertainty values (see Table 5) for pressures $9 \cdot 10^{-4} \text{ Pa} \leq p \leq 0.09 \text{ Pa}$ would have been lower by about a factor of 2.

From Table 14 it can be seen that both NPL and PTB were able to perform the measurements at $3 \cdot 10^{-4} \text{ Pa}$ with an uncertainty of $< 0.65\%$ successfully (in the sense of agreement with the reference value). This uncertainty value was only moderately higher than the one at 0.9 Pa. From this it can be concluded that the SRG is a suitable transfer standard even for such low pressure.

Unfortunately, only the highest target pressure could be linked to a CCM comparison. A second CCM comparison with a range from $3 \cdot 10^{-6} \text{ Pa}$ to $9 \cdot 10^{-4} \text{ Pa}$ was started before this RMO comparison and the measurement taking finished in 2001. This comparison could create the link to the lowest two target pressures of this comparison. Draft A, however, is still in preparation.

The linking at 0.9 Pa to CCM.P-K4 was surprisingly meaningful, since a high correlation of the results of the three NMIs participating in both comparisons could be observed. The relative differences of the weighted mean of the generated pressures of these 3 NMIs to the reference pressure in the two comparisons (Eq. (38)) were so close that a formal linking seemed not to be necessary. Equivalence with the reference value in this comparison automatically means equivalence with the reference value in the CCM.P-K4 and vice versa.

14. Appendix

Suppose we have two measured quantities x_i ($i=1, n=2$) and would like to calculate the weighted mean y and its uncertainty $u(y)$ when the uncertainties $u(x_i)$ are given.

If the x_i are all independent, the results are:

$$y = \frac{\sum_{i=1}^n \frac{x_i}{u^2(x_i)}}{\sum_{i=1}^n \frac{1}{u^2(x_i)}} \quad (43)$$

$$u^2(y) = \frac{1}{\sum_{i=1}^n \frac{1}{u^2(x_i)}} \quad (44)$$

When the x_i are correlated, the following notes may be useful. Suppose we have the model

$$x_i = \frac{p_i}{p_{st}} \quad (45)$$

and the p_i (relative uncertainty u_i) and p_{st} (u_0) are independent, so that

$$u^2(x_i) = u_0^2 + u_i^2 \quad (46)$$

(all uncertainties relative).

Under the assumption that

$$\frac{p_i^2 - p_i p_k}{p_{st}^2} \ll \frac{u_i^2}{u_0^2} \quad i \neq k \quad i, k = 1, 2 \quad (47)$$

which is always the case in the calculations here, because $p_i \approx p_k$ the results are

$$y = \frac{\sum_{i=1}^n \frac{x_i}{u_i^2}}{\sum_{i=1}^n \frac{1}{u_i^2}} \quad (48)$$

$$u^2(y) = u_0^2 + \frac{1}{\sum_{i=1}^n \frac{1}{u_i^2}} \quad (49)$$

These equations make the evaluations easier and better understandable.

15. References

- [1] T. Takaishi, Y. Sensui, Thermal transpiration effect of hydrogen, rare gases and methan, *Trans. Faraday Soc.* **59** (1963), 2503...2514.
- [2] A. Calcatelli, G. F. Molinar, The primary pressure scale in Italy from 10^{-6} Pa to 10^9 Pa'', in *Basic Metrology and Applications*, ed., Levrotto e Bella –Torino 1994.
- [3] M. Bergoglio, A. Calcatelli, Vacuum measurement and traceability in Italy, *Proc. XIV IMEKO World Congress*, Tampere, June 1997.
- [4] K. Jousten, G. Rupschus, The uncertainties of calibration pressures at PTB, *Vacuum* **44** (1993), 569-572.
- [5] K. Jousten, P. Röhl, V. A. Contreras, Volume ratio determination in static expansion systems by means of a spinning rotor gauge, *Vacuum*, **52** (1999), 491...499.
- [6] J. K. Fremerey, Spinning rotor gauges, *Vacuum* **32** (1982), 685...690.
- [7] S. Dittmann, B.E. Lindenau, C.R. Tilford, The molecular drag gauge as a calibration standard, *J. Vac. Sci. Technol. A* **7** (1989), 3356...3360.

- [8] P.Röhl and W. Jitschin, Performance of the SRG with a novel transport device as a transfer standard for high vacuum, *Vacuum* **38** (1988), 507...509.
- [9] G. Messer et al., Intercomparison of nine national high-vacuum standards under the auspices of the BIPM, *Metrologia* **26** (1989), 183.
- [10] K. Jousten, Is the effective accommodation coefficient of the spinning rotor gauge temperature dependent?, *J. Vac. Sci. Technol. A* **21**(1) (2003), 318...324.
- [11] R. Kacker and A. Jones, On use of Bayesian statistics to make the "Guide to the expression of uncertainty in measurement" consistent, *Metrologia* **40** (2003), 235 ... 248.
- [12] Guidelines for CIPM key comparisons, Appendix F of the MRA, March 1999, <http://www.bipm.fr>.
- [13] K. Jousten et al., *J. Vac. Sci. Technol. A* **15** (1997), 2395-2406.
- [14] A.P. Miiller et al., Final report on key comparison CCM.P-K4 of absolute pressure standards from 1 Pa to 1000 Pa, *Metrologia* **39** (2002), Techn. Suppl., 07001.
- [15] M. G. Cox, The evaluation of key comparison data, *Metrologia* **39** (2002), 589...595.
- [16] Guide to the expression of uncertainty in measurement, BIPM, ISO, 1993, ISBN 92-96-10188-9.
- [17] C. Elster, A. Link, and W. Wöger, Proposal for linking the results of CIPM and RMO key comparisons, *Metrologia* **40** (2003), 189...194.
- [18] F. Delahaye and T.J. Witt, Linking the Results of Key Comparison CCEM-K4 with the 10 pF results of EUROMET Project 345, *Metrologia* **39** (2002), Tech. Suppl. 01005.